PHYSICAL REVIEW B VOLUME 32, NUMBER 7 1 OCTOBER 1985

Radiation from fast charged particles in crystals: Unified quantal treatment

Gershon Kurizki
School of Chemistry, Tel Aviv University, Ramat Aviv, 69978 Tel Aviv, Israel

J. K. McIver
Institute for Modern Optics, Department of Physics and Astronomy, University of New Mexico, Albuquerque, New Mexico 87131

(Received 8 February 1985)

We present a unified quantal treatment of the various types of radiation emitted by fast, charged, spin-$\frac{1}{2}$ or spinless particles which propagate at small angles relative to a set of principal atomic planes or rows in a crystal. [Henceforth, direction(s) parallel or perpendicular to these rows (planes) will be referred to as longitudinal or transverse, respectively.] We analyze the dependence of the emission frequencies and rates on the energy and transverse momentum of the incident particle, distinguishing between two fundamental emission modes. One is the transverse mode (TM), which unifies all radiative transitions that are characterized only by the projected potential (i.e., the periodic transverse variation of the crystal potential), such as channeling, quasichanneling, and TM coherent bremsstrahlung transitions. The other one is the longitudinal mode (LM), which includes all transitions involving longitudinal momentum transfer to the lattice, with or without a simultaneous projected potential transition. Our treatment reduces the input needed for a comprehensive analysis of *both* TM and LM emission spectra to the set of Bloch eigenfunctions and quasimomenta of the particle which are obtained on considering its interaction with the projected potential only. The resulting expressions for LM emission rates as a function of the frequency and direction of emission give a considerably more complete and quantitatively correct characterization of this emission mode than previous attempts. Contrary to previous works, we analyze explicitly the effects of quantum recoil r_q, which is the ratio of the photon energy to the incident particle energy. The case of $r_q \sim 1$ [which is applicable to LM emission from electrons and positrons (β particles) with energies as low as few tens of MeV and to TM coherent bremsstrahlung from β particles with energies in the GeV range] is shown to correspond to frequencies, linewidths, and directional distribution of the emission that differ strongly from those obtained in the more familiar limit of $r_q \simeq 0$. Quantum-recoil corrections to emission frequencies given by extant theories are shown to be significant even for r_q considerably smaller than 1.

I. INTRODUCTION

The radiation generated by electrons and positrons with kinetic energies ranging from about 50 keV up to a few GeV (hereafter referred to as fast β particles) as they propagate through crystals has been extensively investigated in recent years.[1–33] Most of the experimental and theoretical work in this field has dealt with radiation from relativistic particles injected into crystals at small angles (up to a few degrees) with respect to a set of principal atomic planes or rows (low-index symmetry planes or axes). The spectrum of this radiation consists of a series of peaks at x-ray or γ-ray wavelengths superimposed on a broad background.[1–22]

The "traditional" approach to the analysis of the spectrum of this radiation is based on the assumption that the propagation of the emitting particle is virtually unaffected by the variation of the potential parallel to the atomic planes (rows). Consequently, the effective potential governing the emission of this radiation is assumed to be the projected potential[34–36] obtainable on averaging the crystal potential over the coordinates of these planes (rows). The projected potential, which varies periodically in the directions(s) transverse to the planes (rows), defines the spectrum of transverse-energy states (or, classically, the transverse trajectories) available to the particle. The radiation spectrum is analyzed quantum mechanically by considering separately the types of radiation described in Table I, each resulting from transitions between transverse-energy states of a particular dynamical regime of the particle.

A number of works have drawn attention to phenomena that are not taken into account by the prevailing models mentioned in Table I.

(1) The assumption that the projected potential governs the emission of radiation has been shown to ignore nonnegligible emission at wavelengths determined by the longitudinal periodicity of the potential, i.e., its periodicity in the planes (rows) along which the particles propagate. This type of emission, hereafter referred to as longitudinal-mode (LM) emission, has been predicted by several authors[25–28] to exist in various dynamical regimes of β particles and has been recently detected by Spence and co-workers, using electrons with kinetic energies of 40–120 keV.[29,30] A general quantal procedure for the evaluation of LM emission intensity has been formulated by us.[31,32] However, as yet the spectrum of this radiation has not been well understood theoretically, as will be shown here.

(2) Adishchev *et al.*[33] have shown experimentally, using highly relativistic electrons, that the spectrum of quasichanneling radiation (QCR) and coherent bremsstrahlung (CB) as a function of the angle of incidence of the particle with respect to a principal atomic row cannot be ade-

TABLE I. Characteristics of commonly investigated types of radiation from fast charged particles in crystals and their prevailing theoretical description.

Characteristics \ Type of radiation	Channeling radiation (CR)[a]	Quasichanneling radiation (QCR)[b]	Coherent bremmsstrahlung (CB)[c]	Pendulum (rendellösung) radiation (PR)[d]
Energies of of emitting β particles	MeV to GeV	MeV to GeV	Tens of keV to tens of GeV	Tens of keV to hundreds of keV
Contributing transverse energy (TE) states	Transversely bound states (below the projected potential maxima)	Transversely unbound states, slightly above the projected potential maxima	Transversely unbound states in the TE continuum (high above the projected potential maxima)	Bound or unbound states of dynamically diffracted particles
Prevailing analytical models for the radiative transitions	(1) Kumakhov's model[e]—transitions between bound TE states of the Lindhard isolated potential well[f]	Scattering of the particle by the Coulomb potential of an isolated atomic row[h]	(1) Überall's model[i] (cf. Ref. 26)—Born approximation scattering of a plane-wave particle by the projected potential	Transitions across the band gap in the two beam (two Bloch waves) approximation[d]
	(2) Estimates of bandwidth imposed on CR lines by the projected potential periodicity for electrons (parabolic crests)[g]		(2) Essentially equivalent (albeit more detailed) quantal[j] and semiclassical[k] treatments	
Features unaccounted for by these models	The projected potential periodicity strongly broadens CR lines corresponding to positron transitions between states slightly below the potential maxima[l]	The distinct TE band structure of unbound states[m] is incompatible with the isolated row model	The Born approximation does not predict correctly the location of certain peaks[n]	No explanation as to why PR lines have not been identified experimentally

[a]References 1 and 4–9.
[b]References 1 and 15.
[c]References 1 and 17–22.
[d]References 23 and 24.
[e]References 10–13.
[f]References 37 and 38.
[g]Reference 9.
[h]Reference 15.
[i]Reference 17.
[j]References 6, 18 and 19.
[k]Reference 20.
[l]References 7 and 14.
[m]References 14 and 16.
[n]References 21 and 22.

quately described by existing analytical models. This has led them to conclude, similarly to other authors[14,26] who have noted the difficulties in interpreting certain spectral features (cf. Table I), that a new, unified theoretical approach to the various types of emission is needed.

We present here a unified quantal treatment of all the aforementioned types of radiation, which is based on their common underlying mechanisms: (1) transitions between bands of transverse energy belonging to *any* dynamical regime of the particle and (2) momentum transfer to the crystal given by $\hbar\mathbf{K}$, where $\mathbf{K}$ is a reciprocal lattice vector (RLV) having a component in the direction(s) of the nearly-free-longitudinal propagation of the particle, which is induced by the periodicity of the crystal potential in the longitudinal direction(s). The first mechanism alone gives rise to what will be termed transverse-mode (TM) emission, whereas the combination of both mechanisms produces what will be termed LM emission.

The present treatment is aimed at providing a prescription for a comprehensive, detailed, and systematic mapping of the TM as well as of the LM emission spectra, as a function of the particle energy, direction of incidence, and direction of emission. The required input is the transverse-energy spectrum and the set of the projected-potential Bloch eigenfunctions. In subsequent parts of this series, the present treatment will be applied to several dynamical regimes of the particle, for which this input is given analytically in a recent paper by Kurizki.[39] The use of this input entails the prediction of new spectral features, notably features demonstrating the close connection of CB with QCR in transitions between unbound transverse-energy states.[32]

The predictions of the present treatment that are apparent, even without considering specific particle regimes, extend those of previous works mainly with regard to the following issues.

(a) Our expressions for emission frequencies and rates apply to all photon energies of interest, including energies comparable to the initial particle energy, i.e., the large-quantum-recoil limit, which has been insufficiently explored hitherto. This is especially important for the characterization of the energetic LM emission spectrum, where the large quantum-recoil limit applies to emitting β particles with energies exceeding a few tens of MeV, which are commonly utilized experimentally [the large-quantum-recoil limit is presently achievable also for TM CB and channeling radiation (CR)—cf. Sec. III]. In the small-quantum-recoil limit, too, our expressions for the emission frequencies yield features that have not been accounted for thus far.

(b) Our expressions for LM emission rates employ Bloch eigenfunctions that characterize a particle diffracted in the full three-dimensionally periodic potential. These eigenfunctions are calculated iteratively, starting from the projected-potential eigenfunctions, using a general procedure proposed in Ref. 39. We show here that this procedure, when carried out to second iteration, gives a more comprehensive and accurate characterization of LM emission than previous treatments of longitudinal potential periodicity effects.[28,40]

Section II of this paper is devoted to the derivation of the general formula for the single-photon emission rate from a fast Dirac particle in a *three-dimensionally periodic potential,* taking account of *quantum recoil* and the emission linewidth (caused either by the inelastic scattering of the particle or the finite crystal thickness). In Sec. III we obtain and investigate two unified formulas for the emission frequencies—one is suitable for negligible quantum recoil and takes into account the refractivity of the crystal medium, the other is appropriate for a sizeable quantum recoil. In Sec. IV we obtain detailed expressions for TM and LM emission rates as a function of the emission frequency and direction. Section V summarizes those features of the radiation which emerge from the present analysis.

II. PRINCIPLES OF EMISSION-RATE CALCULATIONS

We consider the emission of a single photon by a fast-charged particle in a crystal. This process constitutes the main contribution to the small overall probability of photon emission at a given frequency by a negative particle, with any energy between a few tens of keV and a few GeV, traversing a crystal whose thickness is up to a few tens of microns.[1,4] The time-independent matrix element for this process, in a first-order quantum-electrodynamics (QED) perturbation treatment[41,42] is proportional to

$$e\int \mathbf{j}_{if}(\mathbf{r})\cdot\mathbf{a}^*(\mathbf{r})d\mathbf{r}\ ,$$

where the integral extends over the crystal volume. e is the particle charge, $\mathbf{j}_{if}(\mathbf{r})$ is the current for the transition between the initial and final particle eigenstates i,f, and $\mathbf{a}^*(\mathbf{r})$ is the part of the photon wave function associated with the photon creation operator.

The form of $\mathbf{a}^*(\mathbf{r})$ in a crystal should, in principle, take account of the finite crystal slab thickness, spatial dispersion due to crystal refractivity, and diffraction and absorption,[15,43] and thus differ from a plane wave. We shall restrict ourselves to isotropic crystals, where the velocity of light c_q is independent of the direction of emission or the polarization. In such crystals, the deviations of the photon wave function from a plane wave will be shown subsequently to have very little bearing upon the radiative features in the important spectral regions, namely, x rays and γ rays. Accordingly, we shall assume that

$$\mathbf{a}^*(\mathbf{r})\propto e^{-i\mathbf{q}\cdot\mathbf{r}}\hat{\mathbf{e}}^*\ ,$$

$\mathbf{q}$ being the photon wave vector and $\hat{\mathbf{e}}$ the polarization unit vector.

As a first step in our unified treatment, we can now write the following general expression for the emission rate $dW(\mathbf{q})$ summed over photon polarization directions, which is valid for all the types of radiative transitions considered in Sec. I. This expression is derived using basic QED formulas [Eqs. (19-1), (19-2), and (D-1) in Ref. 42, and Eq. (45.4) in Ref. 41]:

$$\frac{dW(\mathbf{q})}{d\Omega_{\hat{\mathbf{q}}}}=\rho_e\frac{V_{\rm crys}}{2\pi\hbar}e^2(c_q/c)q\sum_i\sum_f P_iP_f\frac{1}{1-\boldsymbol{\beta}_{0f}\cdot\hat{\mathbf{q}}}\,|\,\hat{\mathbf{q}}\times\mathbf{j}_{\rm if}(\mathbf{q})\,|^2\,, \tag{1}$$

where, for spin-$\frac{1}{2}$ particles (β particles, protons, muons),

$$\mathbf{j}_{\rm if}(\mathbf{q})=\int d\mathbf{r}\,e^{-i\mathbf{q}\cdot\mathbf{r}}\begin{bmatrix}\Phi_f^*(\mathbf{r}) & \dfrac{c\boldsymbol{\sigma}\cdot\mathbf{p}}{E_f+mc^2}\Phi_f^*(\mathbf{r})\end{bmatrix}\begin{bmatrix}0 & \boldsymbol{\sigma}\\ \boldsymbol{\sigma} & 0\end{bmatrix}\begin{bmatrix}\Phi_i(\mathbf{r})\\ \dfrac{c(\boldsymbol{\sigma}\cdot\mathbf{p})}{E_i+mc^2}\Phi_i(\mathbf{r})\end{bmatrix}. \tag{2}$$

Here, $\mathbf{0}$ and $\boldsymbol{\sigma}$ denote the 2×2 zero matrix and the three 2×2 Pauli matrices, respectively, $\Phi_i(\mathbf{r})$ and $\Phi_f(\mathbf{r})$ are the initial and final eigenstate spinors, E_i and E_f are the initial and final particle energies, and $\mathbf{p}$ is the momentum operator. In Eq. (1), $d\Omega_{\hat{\mathbf{q}}}$ is the solid angle element in the direction of emission specified by unit vector $\hat{\mathbf{q}}$ ρ_e is the density of the particle beam, $V_{\rm crys}$ is the crystal volume, P_i are the probabilities to populate initial Bloch eigenstates i by the incident particle, taken to be a plane wave with momentum $\hbar\mathbf{k}_{0i}$ and energy E_i. The probabilities P_f to obtain particle plane waves leaving the crystal with momenta $\hbar\mathbf{k}_{0f}$ and energy

$$E_f=[(\hbar ck_{0f})^2+m^2c^4]^{1/2}=E_i-\hbar c_q q \tag{3}$$

are determined by matching them on the exit face of the crystal with final Bloch eigenstates which contribute to the emission of the photon with wave vector $\mathbf{q}$. For each $\mathbf{k}_{0f}$, the factor $(1-\boldsymbol{\beta}_{0f}\cdot\hat{\mathbf{q}})^{-1}$, where

$$\boldsymbol{\beta}_{0f}=\hbar c\mathbf{k}_{0f}/E_f \tag{4}$$

arises from the final density-of-states factor as given by Feynman [Eq. (D-1) in Ref. 42]. The discrete summation over the possible outgoing particle momenta in Eq. (1) and the applicability of Feynman's formula result from the discrete nature of momentum exchange of the particle with the crystal, and are contingent on the assumption that momentum is conserved in the emission act (deviations from momentum conservation will be discussed later).

The factor $(1-\boldsymbol{\beta}_{0f}\cdot\hat{\mathbf{q}})^{-1}$ can be recast in an approximate form, which accounts explicitly for the dependence of the emission rate on the quantum recoil

$$r_q=\hbar c_q q/E_i\,, \tag{5}$$

and is valid for r_q sufficiently below 1, so that the outgoing particle is still fast (i.e., β_{0f} is comparable to 1):

$$\frac{1}{1-\boldsymbol{\beta}_{0f}\cdot\hat{\mathbf{q}}}\simeq\frac{1-r_q}{1-\boldsymbol{\beta}_{0i}\cdot\hat{\mathbf{q}}}\,, \tag{6}$$

where

$$\beta_{0i}=\hbar c\mathbf{k}_{0i}/E_i\,. \tag{7}$$

A factor similar to Eq. (6) has not been included in previous attempts to treat CR in the limit of significant r_q values. For $r_q\ll1$, we recover the standard expression for the emission rate.[1–3,6,13] The standard expression becomes totally inappropriate for

$$r_q\lesssim1-1/\gamma_i\,,$$

where

$$\gamma_i=E_i/mc^2\,, \tag{8}$$

i.e., for photons carrying away most of the particle energy, since Eq. (6) then implies that a strong quenching of the emission rate takes place. The behavior very close to $r_q=1-1/\gamma_i$ ($\beta_{0f}\simeq0$) will not be discussed here. It is describable as an inverse photoelectron effect, because in this case the particle, having lost almost all its kinetic energy to the photon, may become trapped in the crystal potential.[44]

Our investigation will henceforth focus on the evaluation of

$$|\mathcal{M}_{\rm if}(\mathbf{q})|^2\equiv\overline{|\,\hat{\mathbf{q}}\times\mathbf{j}_{\rm if}(\mathbf{q})\,|^2}\,, \tag{9}$$

to which the emission rate for a given $\mathbf{q}$ is proportional. Here, the overbar denotes averaging over initial spin polarizations and summation over final spin polarizations. Employing the factorization of $\Phi(\mathbf{r})$ in Eq. (2) into a constant spinor χ and a Klein-Gordon eigenfunction $\psi(\mathbf{r})$ of the particle in the crystal potential, which is valid because of the negligibility of spin-orbit coupling for fast-charged particles in crystals,[45,46] we obtain, after some manipulations

$$\begin{aligned}|\mathcal{M}_{\rm if}(\mathbf{q})|^2&=\frac{\mathcal{A}_i^2\mathcal{A}_f^2}{(1+1/\gamma_i)^2}\left|\chi_f^\dagger\left[\left[2+\frac{r_q}{2-r_q}\right]\mathbf{M}_{\rm if}(\mathbf{q})+\frac{ir_q}{2-r_q}(\boldsymbol{\sigma}\times\mathbf{M}_{\rm if}(\mathbf{q})\right]\chi_i\right|^2\\
&=\frac{\mathcal{A}_i^2\mathcal{A}_f^2}{(1+1/\gamma_i)^2}\left[\left[2+\frac{r_q}{2-r_q}\right]^2\left[|\,M_{\rm if}\,|^2-\sum_{j,j'}\cos\theta_j\cos\theta_{j'}'(M_{\rm if})_j(M_{\rm if})_{j'}'^*\right]\right.\\
&\quad\left.+\frac{r_q^2}{(2-r_q)^2}\left[2\,|\,M_{\rm if}\,|^2-\sum_j|\,M_{\rm if}\,|_j^2\sum_{j'\,(\neq j)}\cos^2\theta_{j'}'+\sum_{\substack{(j\neq j')\\ j,j'}}(M_{\rm if})_j(M_{\rm if})_{j'}'^*\cos\theta_j\cos\theta_{j'}'\right]\right].\end{aligned} \tag{10}$$

Here,

$$\mathscr{A}_i=\left[\frac{1+1/\gamma_i}{2}\right]^{1/2},\qquad \mathscr{A}_f=\left[\frac{1+1/[\gamma_i(1-r_q)]}{2}\right]^{1/2} \tag{11}$$

[these expressions for $\mathscr{A}_i,\mathscr{A}_f$ are obtained neglecting $V(\mathbf{r})/E_i$, $V(\mathbf{r})/E_f$, where $V(\mathbf{r})$ is the crystal potential],

$$\mathbf{M}_{\rm if}(\mathbf{q})=\int d\mathbf{r}\, e^{-i\mathbf{q}\cdot\mathbf{r}}\psi_f^*(\mathbf{r})\frac{\mathbf{p}}{mc\gamma_i}\psi_i(\mathbf{r}) , \tag{12}$$

and

$$\hat{\mathbf{q}}=\sum_{j=x,y,z}\cos\theta_j\,\hat{\mathbf{j}} . \tag{13}$$

The part of $|\mathscr{M}_{\rm if}(\mathbf{q})|^2$ that is proportional to $[2+r_q/(2-r_q)]^2$ arises from the spin-invariant (SI) term $[\chi_f^\dagger\mathbf{M}_{\rm if}(\mathbf{q})\chi_i]$, which requires $\chi_f=\chi_i$ and is the same for spin-$\frac{1}{2}$ and spinless particles (e.g., charged pions). We can rewrite it as follows:

$$|\mathscr{M}_{\rm if}(\mathbf{q})|^2_{\rm SI}=\frac{\mathscr{A}_i^2\mathscr{A}_f^2}{(1+1/\gamma_i)^2}\left[2+\frac{r_q}{2-r_q}\right]^2|M_{\rm if}|^2 \times[1-(\hat{\mathbf{q}}\cdot\hat{\mathbf{M}}_{\rm if})^2] , \tag{14}$$

$\hat{\mathbf{M}}_{\rm if}$ being a unit vector along $\mathbf{M}_{\rm if}$. The part of $|\mathscr{M}_{\rm if}(\mathbf{q})|^2$ proportional to $r_q^2/(2-r_q)^2$ results from spin-photon coupling. It can be seen that in the large-quantum-recoil limit, this part alters the dependence of the emission rate on $\hat{\mathbf{q}}$ compared with that given by Eq. (14). This effect, as well as the comparison of Eq. (10) with currently used formulas[1] will be further discussed in Sec. IV.

In discussing the character of the eigenfunctions $\psi_i(\mathbf{r})$, $\psi_f(\mathbf{r})$, which determine $\mathbf{M}_{\rm if}(\mathbf{q})$, we shall distinguish between two generic geometries. Assuming that the surfaces $z=\pm L/2$ of the crystal slab are perpendicular to a RLV set $g_z\hat{\mathbf{z}}$ and parallel to a RLV set $\mathbf{G}=g_x\hat{\mathbf{x}}+g_y\hat{\mathbf{y}}$, these geometries are

$$\mathbf{r}_\perp\equiv(x,y),\quad k_{0\parallel}\equiv k_{0z}\gg|k_{0\perp}|\equiv|k_{0x}\hat{\mathbf{x}}+k_{0y}\hat{\mathbf{y}}| , \tag{15a}$$

i.e., propagation nearly along the crystal axis z, hereafter referred to as the cross-grating geometry (CGG) (Ref. 34) and

$$\mathbf{r}_\perp\equiv\mathbf{x},\quad |\mathbf{k}_{0\parallel}|\equiv|k_{0z}\hat{\mathbf{z}}+k_{0y}\hat{\mathbf{y}}|\gg|k_{0\perp}|\equiv|k_{0x}| , \tag{15b}$$

i.e., propagation nearly along the crystal plane y-z, hereafter referred to as the systematic reflections geometry (SRG).[34,35]

We neglect surface effects and ignore for the moment inelastic scattering by crystalline degrees of freedom. The Klein-Gordon eigenfunctions then satisfy, to first order in $V(r)/E$ (cf. Refs. 39 and 47–49),

$$[k_0^2-U(\mathbf{r})+\nabla^2]\psi_{\mathbf{k}^{\{n\}}}(\mathbf{r})=0 , \tag{16}$$

where

$$k_0=\frac{mc\gamma}{\hbar}(1-1/\gamma^2)^{1/2},\quad U(\mathbf{r})=\frac{2m\gamma}{\hbar^2}V(\mathbf{r}) . \tag{17}$$

They have the Bloch form and are normalized to 1 in the entire crystal. The quasimomentum $\hbar\mathbf{k}^{\{n\}}$ is determined by the continuity requirement at the surface $z=-L/2$ to have the form[47–49]

$$\hbar\mathbf{k}^{\{n\}}=\hbar(k_{0x}\hat{\mathbf{x}}+k_{0y}\hat{\mathbf{y}}+k_z^{\{n\}}\hat{\mathbf{z}}) . \tag{18}$$

Because the longitudinal propagation of the particle is nearly free, the set of quantum numbers $\{n\}$ labels the eigenvalues of transverse energy $\epsilon_\perp^{\{n\}}$ in the projected potential[34,35]

$$\bar{U}(\mathbf{r}_\perp)=\sum_{\mathbf{g}_\perp}U_{\mathbf{g}_\perp}e^{i\mathbf{g}_\perp\cdot\mathbf{r}_\perp} , \tag{19}$$

which are given by (cf. Ref. 39)

$$\epsilon_\perp^{\{n\}}=k_{0\perp}^2+\delta\epsilon_\perp^{\{n\}},\qquad \delta\epsilon_\perp^{\{n\}}=k_0^2-(k^{\{n\}})^2=k_{0z}^2-(k_z^{\{n\}})^2 . \tag{20}$$

In the CGG these $\{n\}$ specify a two-dimensional band structure, whereas in the SRG a single n labels each band.[35,47–49]

The Bloch eigenfunctions (Bloch waves) of Eq. (16), with $U(\mathbf{r})$ replaced by the reduced projected potential $\bar{U}(\mathbf{r}_\perp)$, are successfully used to analyze the observed diffraction patterns of transversely bound (channeled) as well as unbound β particles with energies between a few tens of keV and a few MeV, in the SRG and the CGG.[47–52] These Bloch waves are also extensively used to evaluate the spectral distribution of CR (only numerically, in quantitative treatments[5–8,14]) emitted by β particles with energies up to a few tens of MeV. When studying CR from β particles with higher energies, the bound Bloch waves are replaced by single-channel (isolated-well) eigenfunctions.[1–4,10–14] For CB analysis, the form of quasifree Bloch waves that is commonly used[6,19] yields results equivalent to the Born approximation[17,18,26] (see the criticism in Sec. I).

Our approach is to retain the full three-dimensionally periodic $U(\mathbf{r})$ when calculating the Bloch eigenfunctions of Eq. (16), since only these eigenfunctions can accurately yield the $\mathbf{M}_{\rm if}(\mathbf{q})$ for all types of radiation and allow their unified description. The limitations of prevailing models for each type of radiation (e.g., the models for CR and CB mentioned above) can be clearly inferred from such a description (cf. Refs. 39 and 32). To show explicitly the consequences of retaining the full $U(\mathbf{r})$ in Eq. (16), we Fourier decompose $\psi_{\mathbf{k}^{\{n\}}}(\mathbf{r})$ in terms of all RLV's $\mathbf{g}$, including RLV's with longitudinal components ($\mathbf{g}_\parallel\neq\mathbf{0}$):

$$\psi_{\mathbf{k}^{\{n\}}}(\mathbf{r})=\frac{1}{V_{\rm crys}^{1/2}}\sum_{\mathbf{g}}c_{\mathbf{g}}^{\{n,\mathbf{k}\}}e^{i(\mathbf{k}^{\{n\}}+\mathbf{g})\cdot\mathbf{r}} , \tag{21}$$

the Fourier coefficients $c_{\mathbf{g}}^{\{n,\mathbf{k}\}}$ being normalized by

$$\sum_{\mathbf{g}}|c_{\mathbf{g}}^{\{n,\mathbf{k}\}}|^2=1 . \tag{22}$$

On substituting Eq. (21) into Eq. (12), while still ignoring inelastic scattering and the finiteness of the crystal slab, we obtain

$$\mathbf{M}_{\rm if}^{(\mathbf{k})}(\mathbf{q})=\left[\beta_i^{\{n_i\}}\sum_{\mathbf{g}} c_{\mathbf{g}}^{\{n_i,\mathbf{k}_i\}}(c_{\mathbf{g}+\mathbf{K}}^{\{n_f,\mathbf{k}_f\}})^* + \sum_{\mathbf{g}}\beta_{\mathbf{g}} c_{\mathbf{g}}^{\{n_i,\mathbf{k}_i\}}(c_{\mathbf{g}+\mathbf{K}}^{\{n_f,\mathbf{k}_f\}})^*\right] \times\delta(\mathbf{k}_i^{\{n_i\}}-\mathbf{k}_f^{\{n_f\}}-\mathbf{K}-\mathbf{q}) , \tag{23}$$

where

$$\beta_{\mathbf{g}}=\frac{\hbar\mathbf{g}}{mc\gamma_i},\quad \beta_i^{\{n_i\}}=\frac{\hbar\mathbf{k}_i^{\{n_i\}}}{mc\gamma_i} , \tag{24}$$

and $\beta_f^{\{n_f\}}$ is defined analogously. Here, $\mathbf{K}$ is a RLV which determines the momentum $\hbar\mathbf{K}$ transferred to the lattice in the emission act.

The distinction between the properties of the two fundamental emission modes, i.e., TM (associated with $\mathbf{K}_{||}=\mathbf{0}$) and LM (associated with $\mathbf{K}_{||}\neq\mathbf{0}$) will be analyzed in Secs. III and IV. Anticipating the results of this analysis we note that the longitudinal Fourier coefficients, i.e., those with $(\mathbf{g}+\mathbf{K})_{||}\neq\mathbf{0}$, which are responsible for LM emission, are induced by the longitudinally varying part of the potential $U(\mathbf{r})-\bar{U}(\mathbf{r}_\perp)$;[53] hence the importance of keeping this part of the potential in a comprehensive theory of the radiation.[54]

The conservation of momentum implied by the δ function in Eq. (23), together with energy conservation [Eq. (3)], determine the allowed emission frequencies at a given $\hat{\mathbf{q}}$ (these will be analyzed in Sec. III). It also allows us to make the following substitutions in Eq. (1):

$$\sum_f\rightarrow\sum_{\{n_f\}}\sum_{\mathbf{K}},\quad P_f\rightarrow P_{\{n_f\}}^{(\mathbf{K})} , \tag{25}$$

where $\{n_f\},\mathbf{K}$ extend over all values contributing to the emission of a photon with wave vector $\mathbf{q}$. In what follows, we shall consider crystals where this ideal δ-function limit is to be replaced by a narrow line shape that does not lead to a significant overlap between matrix elements producing $\mathbf{q}$ via different transitions, so that cross terms of the form $\mathbf{M}_{\rm if}^{(\mathbf{K})}(\mathbf{q})\cdot\mathbf{M}_{i'f'}^{*(\mathbf{K}')}(\mathbf{q})$ (where either $\mathbf{K}\neq\mathbf{K}'$ or the labels of the eigenstates i,f differ from those of i',f') can be disregarded when evaluating the emission rate. Then the line shape can be accounted for by multiplying $|\mathscr{M}_{\rm if}^{(\mathbf{K})}(\mathbf{q})|^2$ [cf. Eqs. (10) or (14)] obtained in the δ-function limit by the line-shape factor squared.

It can be easily shown that the accepted treatment of inelastic scattering in high-energy electron diffraction (HEED) (in addition to the inclusion of thermal effects in the Debye-Waller factor[55]) by means of an optical potential $U^I(\mathbf{r})$[56,57] entails the introduction of exponential decay into the Bloch wave

$$\mathbf{k}^{\{n\}}\rightarrow\mathbf{k}^{\{n\}}+i\mu^{\{n,\mathbf{k}_\perp\}}\hat{\mathbf{z}} ,$$

where the decay (absorption) coefficient $\mu^{\{n\mathbf{k}_\perp\}}$ is given, on a first-order perturbative treatment of $U^I(\mathbf{r})$, by

$$\mu^{\{n,\mathbf{k}_\perp\}}\simeq-\int|\psi_{\mathbf{k}^{\{n\}}}(\mathbf{r})|^2\frac{U^I(\mathbf{r})}{2k_{0z}}d\mathbf{r} .$$

For crystals with $L\gg1/\mu^{\{n,\mathbf{k}_\perp\}}$ [which typically implies L of at least a few microns (Ref. 56)], the decay factors $e^{-\mu\{n,\mathbf{k}_\perp\}z}$ of the Bloch waves in $\mathbf{M}_{\rm if}(\mathbf{q})$ cause the δ-function limit of $|\mathbf{M}_{\rm if}(\mathbf{q})|^2$, and thus of $|\mathscr{M}_{\rm if}(\mathbf{q})|^2$, to be replaced by a Lorentzian profile:

$$|\mathscr{M}_{\rm if}^{(\mathbf{K})}(\mathbf{q})|^2\simeq|\mathscr{M}_{\rm if}^{(\mathbf{K})}(\bar{\mathbf{q}})|^2_{\delta\text{ function}}\frac{(\Delta\bar{K}_z)^2}{(\Delta\bar{K}_z)^2+(\Delta K_z)^2} , \tag{26}$$

where

$$\Delta\bar{K}_z=\mu^{\{n_i,\mathbf{k}_{i\perp}\}}+\mu^{\{n_f,\mathbf{k}_{f\perp}\}} , \tag{27}$$

and ΔK_z is the deviation from momentum conservation in the z direction:

$$\Delta K_z=k_{iz}^{\{n_i,\mathbf{k}_{i\perp}\}}-k_{fz}^{\{n_f,\mathbf{k}_{f\perp}\}}-K_z-\bar{q}_z , \tag{28}$$

K_z and $\bar{q}_z$ being the δ-function limit values. As noted by Andersen *et al.*,[58] in order to obtain the correct Lorentzian linewidth $\Delta\bar{K}_z$, one should exclude from $U^I(\mathbf{r})$ the contributions of inelastic scatterers that cause small changes in $\mathbf{k}^{\{n\}}$, because these cannot produce sizeable deviations from $\bar{\mathbf{q}}$. This can be achieved by taking account only of scattering by (a) valence and atomic core electrons, using the tight-binding model,[59] and (b) phonons with wave vectors outside the first Brillouin zone.[60] We propose the use of this procedure for the computation of spectral linewidths, rather than the more accurate procedure developed by Andersen *et al.*,[50] because the former applies to both LM and TM transitions and to all radiative regimes [CR, QCR, TM CB, and pendulum radiation (PR)], whereas the latter applies in its present form to CR only.

The main shortcoming of the proposed phenomenological procedure is that it can yield only the radiation intensities within the spectral peaks (i.e., near the "δ-function limit" lines). Since this procedure yields only the total intensity of the inelastically-scattered particle wave field (the "absorbed" part of the Bloch waves) and not its energy-momentum distribution, it cannot describe the spectrum of the emission resulting from radiative transitions of this wave field. This emission gives rise to the spectral background between peaks and is commonly termed incoherent bremsstrahlung.[1,2,17,18,20]

Inelastic scattering of the emitted photon, which has been considered in the literature,[15,43] will be neglected. This is allowed since the mean absorption length of the radiation at x-ray and γ-ray frequencies, which are our main concern, is 10^3 to 10^2 times larger than $(\mu^{\{n,\mathbf{k}\}})^{-1}$ (Ref. 15).

In crystals with large lateral extent whose thickness is smaller than $(\mu^{\{n,\mathbf{k}\}})^{-1}$ (typically $L\lesssim1$ μm), the conservation of momentum is violated in the z direction, predominantly by the finiteness of L.[6] The z component of the δ function in Eq. (23) is then replaced by $\sin(\Delta K_z L/2)/(\Delta K_z L/2)$, and

$$|\mathscr{M}_{\rm if}^{(\mathbf{K})}(\mathbf{q})|^2\simeq|\mathscr{M}_{\rm if}^{(\mathbf{K})}(\bar{\mathbf{q}})|^2_{\delta\text{ function}}\left[\frac{\sin(\Delta K_z L/2)}{\Delta K_z L/2}\right]^2 , \tag{29}$$

where ΔK_z and $\bar{\mathbf{q}}$ have the same meaning as in Eq. (28).

III. EMISSION FREQUENCIES

A. A unified frequency formula

The combination of energy- and momentum-conservation conditions for absorption-free, infinite crystals [Eqs. (3) and (23)], taken together with Eqs. (18) and (20), yield

$$\omega=\frac{E_i^2-E_f^2}{\hbar(E_i+E_f)}=\frac{\hbar}{2m\gamma_i(1-r_q)}[(\mathbf{k}_{i\|}^{\{n_i,k_{i\perp}\}}-\mathbf{k}_{f\|}^{\{n_f,k_{f\perp}\}})\cdot(\mathbf{k}_{i\|}^{\{n_i,k_{i\perp}\}}+\mathbf{k}_{f\|}^{\{n_f,k_{f\perp}\}})+\epsilon_{\perp}^{\{n_i,k_{i\perp}\}}(E_i)-\epsilon_{\perp}^{\{n_f,k_{f\perp}\}}(E_f)] \ . \tag{30}$$

It is advantageous to rewrite Eq. (30) as follows

$$\omega=c_q q=\frac{1}{1-r_q/2}\left[\Omega_{\rm if}^{(\mathbf{K})}+\tilde{\boldsymbol{\beta}}_{i\|}^{(\mathbf{K}_\|)}\cdot c\mathbf{q}_\|-\frac{\hbar q_\|^2}{2m\gamma_i}\right] . \tag{31}$$

Here we have introduced the following abbreviations:

$$\Omega_{\rm if}^{(\mathbf{K})}=\left[\boldsymbol{\beta}_{i\|}-\frac{\boldsymbol{\beta}_{\mathbf{K}_\|}}{2}\right]\cdot c\mathbf{K}_\|+\frac{\hbar}{2m\gamma_i}[\epsilon_{\perp}^{(i)}(\gamma_i)-\epsilon_{\perp}^{(f)}(\gamma_f)] \tag{32a}$$

and

$$\boldsymbol{\beta}_{i\|}\equiv\boldsymbol{\beta}_{i\|}^{\{n_i,k_{i\perp}\}},\quad \tilde{\boldsymbol{\beta}}_{i\|}^{(\mathbf{K}_\|)}\equiv\boldsymbol{\beta}_{i\|}-\boldsymbol{\beta}_{\mathbf{K}_\|} ,$$
$$\epsilon_{\perp}^{(i)}\equiv\epsilon_{\perp}^{\{n_i,k_{i\perp}\}},\quad \epsilon_{\perp}^{(f)}\equiv\epsilon_{\perp}^{\{n_f,k_{f\perp}\}} , \tag{32b}$$

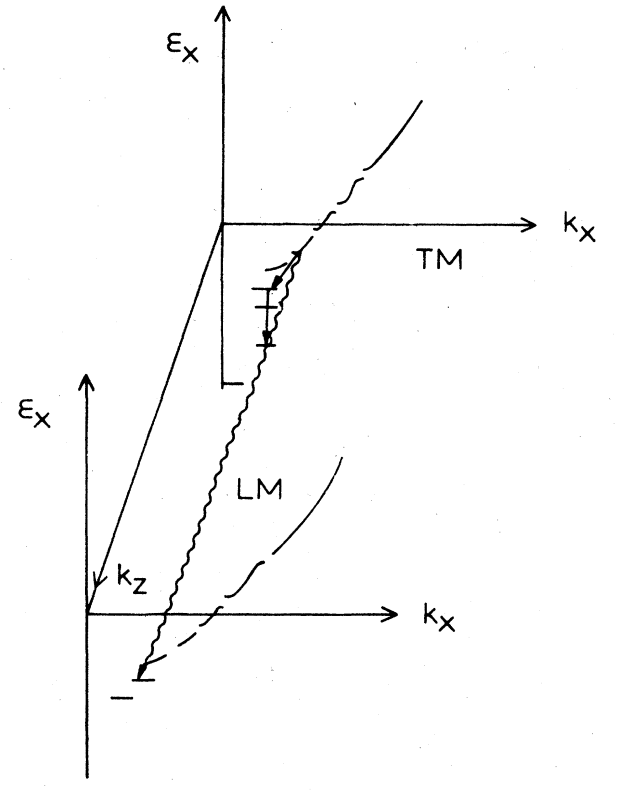

FIG. 1. Modes of radiative transitions of a fast charged particle in a crystal. Solid arrows indicate photons emitted in interband-TM-mode transitions ($\mathbf{K}_\|=0$), wiggly arrow indicates a photon emitted in a combined interband-LM-mode transition ($\mathbf{K}_\|\neq 0$).

$\boldsymbol{\beta}_{i\|}^{\{n_i,k_{i\perp}\}}$ and $\boldsymbol{\beta}_{\mathbf{K}_\|}$ being defined as in Eq. (24) (in what follows, $\tilde{\boldsymbol{\beta}}_{i\|}$ will be shown to determine the Doppler upshift factor for LM emission, whereas a previous attempt[28] has used $\boldsymbol{\beta}_{0i\|}$ instead).

Equation (31) is still implicit, so far as the dependence of ω on $\mathbf{K}$ and the eigenstate parameters is concerned. Its merit is that it provides a framework for the analysis of all possible ω in both the CGG and the SRG, i.e., it is valid for all types of radiation, any value of r_q, and of the refraction index $n_q=c/c_q$. It combines the two basic mechanisms of radiative transitions, namely, longitudinal momentum transfer to the lattice (the first term in $\Omega_{\rm if}^{(\mathbf{K})}$) and transverse-energy change (the second term in $\Omega_{\rm if}^{(\mathbf{K})}$). It should be noted that momentum transfer to the lattice in all three dimensions affects $\Omega_{\rm if}^{(\mathbf{K})}$, as $\mathbf{K}$ accounts for most (*but not all*) of the transverse-energy change causing TM CB and QCR, as will be shown in subsequent parts of this series.

The longitudinal momentum-transfer term in $\Omega_{\rm if}^{(\mathbf{K})}$ is of the order of 10 keV/$\hbar$ for all fast β-particle energies. The transverse-energy-change term ranges from 10 eV/$\hbar$ to a few keV/$\hbar$ for nonrelativistic β particles in all dynamical regimes in the SRG or the CGG. For CR it decreases with γ_i.[1,2,4,6–9] The same ratio between these two terms holds for heavier fast particles. Hence, LM frequencies are expected to be much higher than TM frequencies for the same $\hat{\mathbf{q}}$ and γ_i (Fig. 1).

In what follows, we shall first solve for ω, taking account of crystal refractivity while ignoring r_q, then we shall obtain a solution for ω considering the effects of r_q while keeping $n_q=1$. As will be shown, the domains of validity of each of these solutions can be easily determined in every regime

B. Refractivity effects

In the optical range, we concentrate on emission frequencies satisfying $\omega\ll\omega_p$, ω_p being the plasma frequency of the medium (typically, $\hbar\omega_p\sim$10–20 eV). Then, replacing n_q by a constant $\bar{n}>1$ for transparent media and setting $r_q\simeq 0$, we obtain from Eq. (31)

$$\omega\simeq\frac{\Omega_{\rm if}^{(\mathbf{K})}}{1-\bar{n}\tilde{\boldsymbol{\beta}}_{i\|}\cdot\hat{\mathbf{q}}_\|} . \tag{33}$$

LM emission from fast-charged particles can occur at optical frequencies only for particles heavier than the electron, e.g., muons, pions, and protons at nonrelativistic energies, i.e., $\beta_{i\|}\ll 1$. Such small $\beta_{i\|}$ are usually incompatible with the Čerenkov condition

$$1=\bar{n}(\boldsymbol{\beta}_{i\|}-\boldsymbol{\beta}_{\mathbf{K}_\|})\cdot\hat{\mathbf{q}}_\| ,$$

$|\beta_{\mathbf{K}_{||}}|$ being much smaller than $\beta_{i||}$ for any LM transition having a non-negligible probability (cf. Sec. IV). Therefore, in the optical range, practically only TM emission can satisfy the Čerenkov condition and give rise to the anomalous Doppler effect, i.e., to emission resulting from transitions where $\epsilon_{\perp}^{(i)} < \epsilon_{\perp}^{(f)}$.[61,62]

In the high-frequency ranges, where ω is much larger than ω_p (far uv, x rays, and γ rays), we shall use

$$n_q = n_\omega = 1 - \omega_p^2/2\omega^2 \tag{34}$$

and ignore spatial dispersion corrections to n_ω arising from the interaction of the emitted radiation with the periodic crystal potential.[15,43,63] Such complications of the treatment are unwarranted because the effect of spatial dispersion is to allow emission at the same frequencies as those of LM emission due to the longitudinal modulation of $\psi_{\mathbf{k}\{n\}}(\mathbf{r})$ by the crystal potential, but with a probability smaller by several orders of magnitude than that of the latter process (cf. Sec. IV).

On substituting Eq. (34) into Eq. (31), still assuming $r_q \simeq 0$, we obtain the following formula for high frequencies in polarized media:

$$\omega_{\pm} \simeq \frac{\Omega_{\rm if}^{(\mathbf{K})} \pm [(\Omega_{\rm if}^{(\mathbf{K})})^2 - 2\omega_p^2 (1 - \tilde{\boldsymbol{\beta}}_{i||}^{(\mathbf{K}_{||})'} \cdot \hat{\mathbf{q}}_{||}) \tilde{\boldsymbol{\beta}}_{i||}^{(\mathbf{K}_{||})'} \cdot \hat{\mathbf{q}}_{||}]^{1/2}}{2(1 - \tilde{\boldsymbol{\beta}}_{i||}^{(\mathbf{K}_{||})'} \cdot \hat{\mathbf{q}}_{||})} . \tag{35}$$

This equation implies that two emission frequencies may coexist for the same transition and emission angle. It generalizes the equation obtained previously[64] for CR in the spectral region described by Eq. (34), in that it allows for other types of radiation, including LM emission.

The requirement

$$\Omega_{\rm if}^{(\mathbf{K})} > \sqrt{2}\omega_p [(1 - \tilde{\boldsymbol{\beta}}_{i||}^{(\mathbf{K}_{||})'} \cdot \hat{\mathbf{q}}_{||}) \tilde{\boldsymbol{\beta}}_{i||}^{(\mathbf{K}_{||})'} \cdot \hat{\mathbf{q}}_{||}]^{1/2} , \tag{36}$$

which must be satisfied in order that the roots of Eq. (35) be real, is always obeyed by LM emission from fast β particles. In TM emission, forbidden emission angles or forbidden transitions (at a given emission angle) arise when Eq. (36) is violated. The right-hand side of Eq. (36) attains a maximum value of $\omega_p/\sqrt{2}$ when $\boldsymbol{\beta}_{i||} \cdot \hat{\mathbf{q}}_{||} = \frac{1}{2}$, thereby determining the most probable emission angle to be forbidden for certain TM transitions. In contrast, within the relativistic forward cone $|\hat{\mathbf{q}}_{\perp}| \lesssim 1/\gamma_i$ (discussed in Sec. IV), the right-hand side of Eq. (36) is $\sim \omega_p/\gamma_i$ and, consequently, forbidden TM transitions are much less likely.[2]

In the common case where $\Omega_{\rm if}^{(\mathbf{K})} \gg \omega_p/\gamma_i$ (which includes all LM transitions of relativistic particles), Eq. (35) can be written approximately, for emission within the relativistic cone, as

$$\omega_+ \simeq \frac{\Omega_{\rm if}^{(\mathbf{K})}}{1 - \tilde{\boldsymbol{\beta}}_{i||}^{(\mathbf{K}_{||})'} \cdot \hat{\mathbf{q}}_{||}} - \omega_- , \tag{37}$$

where

$$\omega_- \simeq \omega_p^2/2\Omega_{\rm if}^{(\mathbf{K})} . \tag{38}$$

The branch ω_- is limited in LM emission to $\lesssim \omega_p^2/2cK_{||}$, i.e., it lies in the infrared and therefore its propagation through the crystal cannot be described by Eq. (34). Its only effect is to shift slightly downwards the LM ω_+ (with respect to the values obtained for $n_q = 1$). In contrast, the ω_- branch can be shown from Eq. (38) to grow with γ_i for certain TM transitions, e.g., CR (this follows from the form of $\Omega_{\rm if}$ in this case[6,10]). It can then coexist with the ω_+ branch at relativistic particle energies, as well as shift the ω_+ values considerably downwards relative to their values at $n_q = 1$.

C. Quantum-recoil effects

The effects of quantum recoil r_q on the emission frequencies have not been described explicitly hitherto. A formula containing r_q implicitly has been given for CR.[1]

Solving Eq. (31), on taking account of r_q while assuming $c_q = c$, we obtain

$$\omega = \left[\frac{E_i}{\hbar}\right] \frac{(1 - \tilde{\boldsymbol{\beta}}_{i||}^{(\mathbf{K}_{||})'} \cdot \hat{\mathbf{q}}_{||} - d_\omega)}{\hat{\mathbf{q}}_{\perp}^2} \times \left[1 \pm \left[1 - \frac{2\hbar\Omega_{\rm if}^{(\mathbf{K})}(\gamma_i)\hat{\mathbf{q}}_{\perp}^2}{E_i(1 - \tilde{\boldsymbol{\beta}}_{i||}^{(\mathbf{K}_{||})'} \cdot \hat{\mathbf{q}}_{||} - d_\omega)^2}\right]^{1/2}\right] . \tag{39}$$

Here,

$$\hat{\mathbf{q}}_{\perp}^2 = \sin^2\theta \tag{40a}$$

in the CGG,

$$\hat{\mathbf{q}}_{\perp}^2 = \sin^2\theta \sin^2\phi \tag{40b}$$

in the SRG, the polar axis being directed along z.

The term

$$d_\omega = \frac{\hbar}{2m\gamma_i\omega} [\epsilon_{\perp}^{(f)}(\gamma_i) - \epsilon_{\perp}^{(f)}(\gamma_f)] \tag{41}$$

is a correction to $\hbar\Omega_{\rm if}^{(\mathbf{K})}(\gamma_i)/E_i$, due to the recoil. We can obtain d_ω for several types of radiative transitions, by using the appropriate forms of $\epsilon_{\perp}$ (cf. Ref. 39 and Refs. 34 and 35), then employ it in deriving explicit solutions of Eq. (39) for the following transitions.

(1) If $\{n_f\}$ pertains to a band lying high above the projected potential maxima, then

$$d_\omega \simeq 0 . \tag{42a}$$

(2) If $\{n_f\}$ pertains to a band in the bound transverse-energy region, then

$$d_\omega = -\frac{V_{\rm BH}}{E_i} + \frac{\hbar}{2m\gamma_i\omega} [\Delta\epsilon_{\perp}^{(f)}(\gamma_i) - \Delta\epsilon_{\perp}^{(f)}(\gamma_i(1 - r_q))] , \tag{42b}$$

where $V_{\rm BH}$ is the barrier height of the projected potential (i.e., the difference between its maximum and minimum) and $\Delta\epsilon_{\perp}^{(f)}$ measures $\epsilon_{\perp}^{(f)}$ from the projected potential minimum. For CR transitions that involve $\{n_f\}$ pertaining to bands close to the projected potential minimum, the second term in Eq. (42b) is much smaller than the first

one. Hence, we may solve Eq. (39) iteratively in this case, using $d_\omega = -V_{\rm BH}/E_i$ in the first iteration. We then substitute the resulting ω and r_q into Eq. (42b) to obtain d_ω, which is then used to obtain the second-iteration solution for ω.

(3) For all LM transitions $|d_\omega| \ll \hbar\Omega_{\rm if}^{(\mathbf{K})}/E_i \simeq \beta_{K_\parallel}$. Hence, a similar iterative solution of Eq. (39) may be obtained in this case, using $d_\omega = 0$ in the first iteration.

An algebraic investigation of Eq. (39) has shown that the upper-branch frequencies always exceed $E_i/\hbar$. Hence, they correspond to transitions from positive- to negative-particle energies, i.e., transitions involving both particles and antiparticles.[41,65] This process is different from the one considered here, namely, photon emission by a *single* particle. Therefore, we shall identify ω in what follows with the *lower branch* of Eq. (39). We have verified that these frequencies are always real and for $\Omega_{\rm if}^{(\mathbf{K})} > 0$, they are always positive.[66] In what follows we summarize the behavior of ω, as obtained from Eq. (39) in the first iteration for several representative cases in the CGG.

1. The range $2\gamma_i^2\hbar\Omega_{\rm if}^{(\mathbf{K})} > E_i$

LM *emission* in this range is allowed only if

$$\theta^2 > \theta_{\min}^2 \gtrsim \frac{(2\beta_{K_z})^{1/2}}{\gamma_i} - \frac{1}{2\gamma_i^2} + \sqrt{2}\beta_{K_z}^{3/2} + \frac{\sqrt{2}}{16\beta_{K_z}^{1/2}\gamma_i^3}\ , \tag{43}$$

otherwise the requirement $\hbar\omega < E_i - mc^2$ is violated. For $2\gamma_i^2\beta_{K_z} \gg 1$, this condition amounts to the entire relativistic forward cone ($|\theta| \lesssim 1/\gamma_i$) being forbidden. At angles satisfying $\beta_{K_z} \gtrsim \theta^2 > \theta_{\min}^2$, the frequency in this case is found to be

$$\omega \simeq \left[\frac{E_i}{\hbar}\right]\left[1 + \frac{1}{2\gamma_i^2\beta_{K_z}}\left[1 - \frac{\theta^2}{2\beta_{K_z}}\right] - \frac{\theta^4}{4\beta_{K_z}^2} + O(\theta^6/\beta_{K_z}^3)\right], \tag{44a}$$

whereas at larger angles, satisfying $1 \gg \theta^2 \gtrsim 2\beta_{K_z}$, ω assumes the form

$$\omega \simeq \frac{2\Omega_{\rm if}^{(\mathbf{K})}(\gamma_i)}{\theta^2}\left[1 + \frac{1}{12\gamma_i^2} - \tfrac{5}{6}\beta_{K_z} - \frac{2\beta_{K_z}}{\theta^2\gamma_i^2}\left[1 + \frac{1}{2\gamma_i^2\beta_{K_z}}\right] + O((\beta_{K_z}/\theta^2)^3)\right]. \tag{44b}$$

CR *emission* is allowed everywhere in the above range (which implies $|d_\omega| \gg 1/\gamma_i^2$). At angles satisfying $|d_\omega| \gtrsim \theta^2$, we obtain

$$\omega \simeq \Omega_{\rm if}(\gamma_i)\left[\frac{1}{|d_\omega|} - \frac{1}{d_\omega^2\gamma_i^2} + \frac{1}{2\gamma_i^2} + |d_\omega| - \frac{1}{2|d_\omega|^3\gamma_i^4} + \theta^2\left[-\frac{1}{3|d_\omega|} + \frac{1}{2d_\omega^2} - \frac{1}{2|d_\omega|^3\gamma_i^2}\right] + O(\theta^4)\right]\left[1 + \frac{\theta^2}{3}\right]. \tag{45a}$$

The leading term here is

$$\Omega_{\rm if}/|d_\omega| \sim (E_i/\hbar)(\hbar\Omega_{\rm if}/V_{\rm BH}) \ll E_i/\hbar\ ,$$

hence, no forbidden angles arise in this case. The corresponding form of ω at $1 \gg \theta^2 \gtrsim |d_\omega|$ is

$$\omega \simeq \frac{2\Omega_{\rm if}(\gamma_i)}{\theta^2}\left[1 - \frac{4|d_\omega|}{\theta^2} - \frac{4d_\omega^2}{\theta^4}\right] \times \left[1 + \frac{2|d_\omega|}{\theta^2} + \frac{1}{\gamma_i^2\theta^2} - \frac{\theta^2}{12}\right]\left[1 + \frac{\theta^2}{3} + \frac{\theta^4}{9}\right]. \tag{45b}$$

TM CB *emission frequencies* in the above range assume the form

$$\omega \sim \left[\frac{E_i}{\hbar}\right]\left[\left[\frac{k_{f\perp}}{k_{i\perp}}\right]^2 + O(\theta^2)\right] \tag{46}$$

and therefore are forbidden at small angles if $(k_{f\perp}/k_{i\perp})^2 > 1 - 1/\gamma_i$.

2. The range $2\gamma_i^2\hbar\Omega_{\rm if}^{(\mathbf{K})} \ll E_i$

In this range (more precisely, for $\gamma_i^2\hbar\Omega_{\rm if}^{(\mathbf{K})} < E_i/8$) we may expand the square root in Eq. (39) (in powers of the second term therein) thus obtaining (for the lower branch of ω)

$$\omega = \frac{\Omega_{\rm if}^{(\mathbf{K})}(\gamma_i)}{1 - \tilde{\boldsymbol{\beta}}_{i\parallel}^{(\mathbf{K}_\parallel)}\cdot\hat{\mathbf{q}}_\parallel - d_\omega}\left[1 - \frac{\hbar\Omega_{\rm if}^{(\mathbf{K})}(\gamma_i)\hat{\mathbf{q}}_\perp^2}{2E_i(1 - \tilde{\boldsymbol{\beta}}_{i\parallel}^{(\mathbf{K}_\parallel)}\cdot\hat{\mathbf{q}}_\parallel - d_\omega)^2}\right] + O((\hbar\Omega_{\rm if}^{(\mathbf{K})}/E_i)^3)\ . \tag{47}$$

Here, the leading term contains the effects of quantum recoil only in d_ω. The second term in the large parentheses is a correction entirely due to quantum-recoil effects. In the CGG, for $1 \gg \theta^2$, the Doppler upshift factor in Eq. (47) assumes the following form:

$$\frac{1}{1 - \tilde{\boldsymbol{\beta}}_{i\parallel}^{(\mathbf{K}_\parallel)}\cdot\hat{\mathbf{q}}_\parallel - d_\omega} \simeq \frac{2\gamma_i^2}{1 + 2\gamma_i^2\beta_{K_z}\left[1 - \frac{\theta^2}{2} + \frac{\theta^4}{24}\right] + \gamma_i^2\theta^2\left[1 - \frac{\theta^2}{12}\right] - 2\gamma_i^2 d_\omega + \frac{\hbar^2\epsilon_\perp^{(i)}}{m^2c^2(1 - 1/\gamma_i^2)}}\ . \tag{48}$$

To illustrate the behavior of ω at $1 \gg \theta^2$ in this range, we write the following results obtained from Eqs. (47) and (48). For LM emission we find

$$\omega \sim \frac{2\gamma_i^2 \Omega_{\rm if}^{(\mathbf{K})}(\gamma_i)}{1+2\gamma_i^2\beta_{K_z}+\gamma_i^2\theta^2}\left[1-\frac{4\gamma_i^4\beta_{K_z}\theta^2}{1+\gamma_i^2\theta^2}\right], \tag{49a}$$

and for CR we find

$$\omega \sim \frac{2\gamma_i^2 \Omega_{\rm if}(\gamma_i)}{1+2\gamma_i V_{\rm BH}/mc^2+\gamma_i^2\theta^2}\left[1-4\gamma_i^4\left[\frac{\hbar\Omega_{\rm if}(\gamma_i)}{E_i}\right]\frac{\theta^2}{1+2\gamma_i V_{\rm BH}/mc^2+\gamma_i^2\theta^2}\right]. \tag{49b}$$

Thus, in the large-recoil limit (corresponding to $2\gamma_i^2\Omega_{\rm if}^{(\mathbf{K})} \gtrsim E_i$), which has not been well understood hitherto, the behavior of ω (as a function of the emission angle, γ_i and $\Omega_{\rm if}$) can differ strongly from that obtained in the more familiar small-recoil limit ($\gamma_i^2\Omega_{\rm if}^{(\mathbf{K})} \ll E_i$). However, even in the latter limit our treatment yields significant corrections to ω, as compared to solutions where recoil effects are disregarded.

In addition to accounting for the effects of r_q, one must include in $\Omega_{\rm if}^{(\mathbf{K})}(\gamma_i)$ the effect of the "transverse recoil" $\mathbf{q}_\perp$. The latter affects $\mathbf{k}_{f\perp}$, as seen from the conservation-of-momentum relation

$$\mathbf{k}_{f\perp}=\mathbf{k}_{i\perp}-\mathbf{K}_\perp-\mathbf{q}_\perp . \tag{50}$$

In turn, $\mathbf{k}_{f\perp}$ affects $\epsilon_\perp^{\{n_f,\mathbf{k}_{f\perp}\}} \equiv \epsilon_\perp^{(f)}$ used in $\Omega_{\rm if}^{(\mathbf{K})}(\gamma_i)$. The transverse-recoil effect manifests the nondipolar nature of most types of radiative transitions, as will be shown in subsequent parts of this series. It has been considered before in the context of CR (Refs. 1–3) and TM CB.[21] Here, we note that for LM emission this effect can be taken into account iteratively: ω is computed in the first iteration using only the longitudinal part of $\Omega_{\rm if}^{(\mathbf{K})}$, then $\omega\hat{\mathbf{q}}/c$ is inserted into Eq. (50) to determine $\mathbf{k}_{f\perp}$. The latter serves to calculate $\epsilon_\perp^{(f)}$ [and thus the full $\Omega_{\rm if}^{(\mathbf{K})}(\gamma_i)$] to be used in the second iteration.

D. Spectral linewidth computation

The deviation from momentum conservation in the z direction, $\hbar\Delta K_z$ [Eq. (28)], which is allowed by inelastic scattering or finite crystal thickness, simply adds on to the δ-function limit momentum transfer $\hbar K_z$. Consequently, ΔK_z causes the following deviation from the value of $\Omega_{\rm if}^{(\mathbf{K})}$ as given by Eq. (32):

$$\Delta\Omega_{\rm if} \simeq \tilde{\beta}_{iz}^{(K_z)} c\,\Delta K_z . \tag{51}$$

This expression can be converted into a frequency deviation $\Delta\omega$ by using Eqs. (35) or (39) and thus allows one to calculate the linewidth of any type of radiation for any amount of quantum recoil. For example, the mean frequency deviation $\Delta\bar{\omega}$ of the Lorentzian profile associated with inelastic scattering in the case of Eq. (44a) is

$$\Delta\bar{\omega} \sim \frac{E_i}{2\hbar\gamma_i^2}\frac{\beta_{\Delta\bar{K}_z}}{\beta_{\bar{K}_z}^2}, \tag{52a}$$

where $\Delta\bar{K}_z$ is given by Eq. (27), whereas in the range of validity of Eq. (47), it has the form

$$\Delta\bar{\omega} \simeq \frac{\tilde{\beta}_{iz}^{(K_z)} c\,\Delta\bar{K}_z}{1-\tilde{\boldsymbol{\beta}}_{i\parallel}^{(\mathbf{K}_\parallel)}\cdot\hat{\mathbf{q}}_\parallel - d_\omega} - \frac{\Omega_{\rm if}^{(\mathbf{K})}(\gamma_i)}{(1-\tilde{\boldsymbol{\beta}}_{i\parallel}^{(\mathbf{K}_\parallel)}\cdot\hat{\mathbf{q}}_\parallel - d_\omega)^3}\left[\frac{\hbar\tilde{\beta}_{iz}^{(K_z)} c\,\Delta\bar{K}_z}{2E_i}\right]\hat{\mathbf{q}}_\perp^2 . \tag{52b}$$

A similar connection between $\Delta\omega$ and ΔK_z holds for the linewidth profile caused by finite thickness [Eq. (29)].

IV. SPECTRAL LINE INTENSITIES

In this section we outline general procedures, valid for all dynamical regimes of the particle in the CGG and the SRG, that allow the explicit evaluation of the emission rate as a function of ω and $\hat{\mathbf{q}}$, according to Eqs. (1) and (10). The analysis in Sec. III has shown that LM transitions give rise to much higher ω than TM transitions, for given $\mathbf{k}_{0i}$ and $\hat{\mathbf{q}}$. There is therefore a need to evaluate separately the transition matrix elements $\mathbf{M}_{\rm if}^{(\mathbf{K}_\perp)}(\mathbf{q})$ and $\mathbf{M}_{\rm if}^{(\mathbf{K}_{\parallel\neq 0})}(\mathbf{q})$ [Eq. (23)] associated with emission at TM and LM frequencies, respectively.

The separate evaluation of these two types of transition matrix elements is based on the possibility of decomposing to a high accuracy (cf Ref. 39) each Bloch wave as follows:

$$\psi_{\mathbf{k}\{n\}}(\mathbf{r}) \simeq \frac{1}{V_{\rm crys}^{1/2}} e^{i\mathbf{k}_\parallel^{\{n,\mathbf{k}_\perp\}}\cdot\mathbf{r}_\parallel}\left[w_{\{n\}\mathbf{k}_\perp}(\mathbf{r}_\perp)+\sum_{\mathbf{h}_\parallel} e^{i\mathbf{h}_\parallel\cdot\mathbf{r}_\parallel}\delta w_{\{n\}\mathbf{k}_\perp}^{(\mathbf{h}_\parallel)}(\mathbf{r}_\perp)\right]. \tag{53}$$

Here,

$$w_{\{n\}\mathbf{k}_\perp}(\mathbf{r}_\perp)=\sum_{\mathbf{g}_\perp} c_{\mathbf{g}_\perp}^{\{n,\mathbf{k}_\perp\}} e^{i(\mathbf{k}_\perp+\mathbf{g}_\perp)\cdot\mathbf{r}_\perp} \tag{54}$$

is the projected potential eigenfunction, satisfying

$$[\epsilon_\perp^{\{n,\mathbf{k}_\perp\}}+\nabla_\perp^2-\bar{U}(\mathbf{r}_\perp)]w_{\{n\}\mathbf{k}_\perp}(\mathbf{r}_\perp)=0 , \tag{55}$$

and being normalized by

$$\int d\mathbf{r}_\perp \,|\, w_{\{n\}\mathbf{k}_\perp}(\mathbf{r}_\perp)\,|^2 = A_{\rm cell} , \tag{56}$$

where $A_{\rm cell}$ is the area of the unit cell in the transverse directions in the CGG, or the systematic-reflections cell period in the SRG. The terms in the summation over $\mathbf{h}_{||}$ have the form

$$e^{i\mathbf{h}_{||}\cdot\mathbf{r}_{||}}\delta w^{(\mathbf{h}_{||})}_{\{n,\mathbf{k}_\perp\}}(\mathbf{r}_\perp)=e^{i\mathbf{h}_{||}\cdot\mathbf{r}_{||}}\sum_{\mathbf{g}_\perp} c^{\{n,\mathbf{k}_\perp\}}_{\mathbf{g}_\perp+\mathbf{h}_{||}} e^{i(\mathbf{k}_\perp+\mathbf{g}_\perp)\cdot\mathbf{r}_\perp}\ , \tag{57}$$

where the summation extends over all $\mathbf{g}_\perp$ such that $\mathbf{g}_\perp+\mathbf{h}_{||}$ are RLV's. These terms express the weak longitudinal modulation of the Bloch wave caused by the longitudinally varying part of the potential $U(\mathbf{r})-\bar{U}(\mathbf{r}_\perp)$. Equation (23) shows that these terms are associated with LM transitions, whereas TM transitions involve the $w_{\{n,\mathbf{k}_\perp\}}$ only.

The procedure outlined in Ref. 39 allows us to evaluate the $\delta w^{(\mathbf{h}_{||})}_{\{n,\mathbf{k}_\perp\}}$ from the projected potential eigenfunctions and eigenvalues $w_{\{n,\mathbf{k}_\perp\}}$ and $\epsilon_\perp^{\{n,\mathbf{k}_\perp\}}$. Using this procedure, we have obtained, as a result of a lengthy analysis summarized in the Appendix, the following approximate form of the LM transition matrix element:

$$\mathbf{M}^{(\mathbf{K}_{||}\neq 0)}_{\rm if}(\mathbf{q})=\mathbf{T}^{(\mathbf{K})}_{\rm if}+\mathbf{Q}^{(\mathbf{K})}_{\rm if}+\mathbf{R}^{(\mathbf{K})}_{\rm if}\ . \tag{58}$$

Here,

$$\mathbf{T}^{(\mathbf{K})}_{\rm if}=-\frac{i\hbar}{mc\gamma_i}\frac{1}{A_{\rm cell}}\int_{\rm cell} d\mathbf{r}_\perp e^{-i\mathbf{q}_\perp\cdot\mathbf{r}_\perp} w_f^*\nabla_\perp \delta w_i^{-(\mathbf{K}_{||})}$$
$$\simeq\chi_{\mathbf{K}_{||}}\left[-\frac{i\hbar}{mc\gamma_i}\right]\frac{1}{A_{\rm cell}}\int_{\rm cell} d\mathbf{r}_\perp e^{-i\mathbf{q}_\perp\cdot\mathbf{r}_\perp}[\nabla_\perp\phi_{-\mathbf{k}_{||}}(\mathbf{r}_\perp)]w_f^* w_i+O(\chi^2_{\mathbf{K}_{||}}\hbar|\langle\nabla_\perp\phi_{-\mathbf{K}_{||}}(\mathbf{r}_\perp)\rangle|/mc\gamma_i)\ , \tag{59}$$

$$\mathbf{Q}^{(\mathbf{K})}_{\rm if}=-\boldsymbol{\beta}_{\mathbf{K}_{||}}\frac{1}{A_{\rm cell}}\int_{\rm cell} d\mathbf{r}_\perp e^{-i\mathbf{q}_\perp\cdot\mathbf{r}_\perp} w_f^*\delta w_i^{-(\mathbf{K}_{||})}$$
$$\simeq-\chi_{\mathbf{K}_{||}}\boldsymbol{\beta}_{\mathbf{K}_{||}}\frac{1}{A_{\rm cell}}\int_{\rm cell} d\mathbf{r}_\perp e^{-i\mathbf{q}_\perp\cdot\mathbf{r}_\perp}\phi_{-\mathbf{K}_{||}}(\mathbf{r}_\perp)w_f^* w_i+O(\chi^2_{K_{||}}\beta_{\mathbf{K}_{||}})\ , \tag{60}$$

and

$$\mathbf{R}^{(\mathbf{K})}_{\rm if}=\boldsymbol{\beta}_{i||}\frac{1}{A_{\rm cell}}\int_{\rm cell} d\mathbf{r}_\perp e^{-i\mathbf{q}_\perp\cdot\mathbf{r}_\perp}\left[(\delta w_f^{(\mathbf{K}_{||})})^* w_i+w_f^*\delta w_i^{(-\mathbf{K}_{||})}+\sum_{\mathbf{h}_{||}(\neq 0)}(\delta w_f^{(\mathbf{h}_{||}+\mathbf{K}_{||})})^*\delta w_i^{(\mathbf{h}_{||})}\right]$$
$$\simeq\chi_{\mathbf{K}_{||}}\frac{\hat{\boldsymbol{\beta}}_{i||}}{\hat{\boldsymbol{\beta}}_{i||}\cdot\mathbf{K}_{||}}\frac{1}{A_{\rm cell}}\int_{\rm cell} d\mathbf{r}_\perp e^{-i\mathbf{q}_\perp\cdot\mathbf{r}_\perp}\phi_{-\mathbf{K}_{||}}(\mathbf{r}_\perp)\left[\left[-\frac{\hbar}{2mc\gamma_i}(\delta\epsilon_\perp^{(i)}+\delta\epsilon_\perp^{(f)})+\beta_K K-\boldsymbol{\beta}_{i\perp}\cdot(\mathbf{K}_\perp+\mathbf{q}_\perp)\right]w_f^* w_i\right.$$
$$+i\left[\boldsymbol{\beta}_{\mathbf{K}_\perp}-\frac{\boldsymbol{\beta}_{i\perp}}{2}+\tfrac{3}{2}\boldsymbol{\beta}_{f\perp}\right]\cdot w_f^*\nabla_\perp w_i\frac{-\hbar}{2mc\gamma_i}w_f^*\nabla_\perp^2 w_i$$
$$\left.+i\boldsymbol{\beta}_{\mathbf{K}_\perp}\cdot(\nabla_\perp w_f^*)w_i+\frac{\hbar}{2mc\gamma_i}(\nabla_\perp w_f^*)\cdot(\nabla_\perp w_i)\right]$$
$$+\boldsymbol{\beta}_{i||}\sum_{\mathbf{g}_{||}(\neq 0)}\chi_{\mathbf{K}_{||}+\mathbf{g}_{||}}\chi_{\mathbf{g}_{||}}\frac{1}{A_{\rm cell}}\int_{\rm cell} d\mathbf{r}_\perp e^{-i\mathbf{q}_\perp\cdot\mathbf{r}_\perp}\phi_{\mathbf{g}_{||}}(\mathbf{r}_\perp)\phi_{-(\mathbf{g}_{||}+\mathbf{K}_{||})}(\mathbf{r}_\perp)w_f^* w_i+O(\chi^3_{\mathbf{K}_{||}}\beta_{i||})\ . \tag{61}$$

Here and hereafter we use the abbreviations

$$w_i\equiv w_{\{n_i,\mathbf{k}_{i\perp}\}},\quad w_f\equiv w_{\{n_f,\mathbf{k}_{f\perp}\}},\quad \hat{\boldsymbol{\beta}}_{i||}=\boldsymbol{\beta}_{i||}/\beta_{i||}\ , \tag{62}$$

$$\phi_{\mathbf{g}_{||}}(\mathbf{r}_\perp)=\sum_{\mathbf{g}_\perp}\phi_{\mathbf{g}_\perp+\mathbf{g}_{||}}e^{i\mathbf{g}_\perp\cdot\mathbf{r}_\perp}$$
$$=\sum_{\mathbf{g}_\perp}(V_{\mathbf{g}_\perp+\mathbf{g}_{||}}/V_{g_m})e^{i\mathbf{g}_\perp\cdot\mathbf{r}_\perp} \tag{63}$$

and

$$\chi_{\mathbf{g}_{||}}=V_{g_m}/\hbar c\boldsymbol{\beta}_{0i||}\cdot\mathbf{g}_{||}\ , \tag{64}$$

where g_m denotes the shortest nonzero RLV and $\chi_{\mathbf{g}_{||}}$ serves as the perturbative expansion parameter in the calculation of $\delta w^{(\mathbf{g}_{||})}_{\{n\mathbf{k}_\perp\}}$ from $w_{\{n\mathbf{k}_\perp\}}$ (cf. the Appendix). For fast β particles, $\chi_{\mathbf{g}_{||}}$ can typically lie in the range between 10^{-2} and 10^{-3}. For protons with kinetic energies up to a few MeV, $\chi_{\mathbf{g}_{||}}$ can exceed 1, in which case longitudinal modulation effects cannot be analyzed by our method (which is contingent on the assumption $|\chi_{\mathbf{g}_{||}}|\ll 1$).

As shown in the Appendix, $R^{(\mathbf{K})}_{\rm if}$ arises from terms in δw that are of order $\chi^2_{\mathbf{K}_{||}},\chi_{\mathbf{g}_{||}}\chi_{\mathbf{g}_{||}+\mathbf{K}_{||}}$, whereas the components $\mathbf{T}^{(\mathbf{K})}_{\rm if}$ and $\mathbf{Q}^{(\mathbf{K})}_{\rm if}$ arise from terms that are linear in $\chi_{\mathbf{K}_{||}}$. However, in $\mathbf{R}^{(\mathbf{K})}_{\rm if}$ these second-order terms in $\chi_{\mathbf{K}_{||}}$ are multiplied by $\beta_{i||}\sim 1$, while the first-order terms in $\chi_{\mathbf{K}_{||}}$ in the other components are multiplied by much smaller factors. Equations (59)–(61) show that $R^{(\mathbf{K})}_{\rm if}$ is comparable to the other two components, and for certain values of the parameters it becomes the largest component. The quasiclassical treatment of LM emission from channeled particles in the CGG by Vedrinskii and Malyshevskii[28] does not contain a term equivalent to $\mathbf{R}^{(\mathbf{K})}_{\rm if}$, nor can this term be obtained from Buxton's[40] formula for the longitudinal modulation of Bloch waves (this

formula is accurate to first order in $\chi_{\mathbf{K}_{||}}$). The use of these treatments therefore significantly underestimates the LM emission rate, especially in cases (discussed below) where the contribution of $\mathbf{R}_{\rm if}^{(\mathbf{K})}$ to $|\mathscr{M}_{\rm if}(\mathbf{q})|^2$ is the leading one.

The TM transition matrix element, which is obtained from Eq. (23) on using Eqs. (50), (53) and (54) and disregarding the small δw contributions, has a much simpler form than its LM counterpart:

$$\mathbf{M}_{\rm if}^{(\mathbf{K}_\perp)}(\mathbf{q})=\frac{1}{A_{\rm cell}}\int_{\rm cell}d\mathbf{r}_\perp e^{-i\mathbf{q}_\perp\cdot\mathbf{r}_\perp}w_f^*(\mathbf{r}_\perp)\times\left[-\frac{i\hbar}{mc\gamma_i}\nabla_\perp+\boldsymbol{\beta}_{i||}\right]w_i(\mathbf{r}_\perp)\ . \quad (65)$$

Using an identity noted by Bird and Buxton,[9] Eq. (65) can be rewritten as follows:

$$\mathbf{M}_{\rm if}^{(\mathbf{K}_\perp)}(\mathbf{q})=(\mathbf{M}_{\rm if}^{(\mathbf{K}_\perp)})_\perp+\frac{\mathbf{q}_\perp\cdot(\mathbf{M}_{\rm if}^{(\mathbf{K}_\perp)})_\perp\boldsymbol{\beta}_{i||}}{\hbar(\epsilon_\perp^{(i)}-\epsilon_\perp^{(f)}+q_\perp^2)/2mc\gamma_i}\ . \quad (66)$$

Inspection of the above expressions for LM and TM transition matrix elements reveals the absence of generally valid selection rules on the values of $\{n_i\}-\{n_f\}$. In TM emission, dipole selection rules are relaxed by nondipolar effects incurred by $\mathbf{q}_\perp$ and by the fact that w_i (or w_f) has no strict parity with respect to $\mathbf{r}_\perp$ unless $k_{i\perp}$ (or $k_{f\perp}$) is a half integer times g_m (i.e., Bragg incidence or exit[34,35]). In LM emission, the nondipolar character is stronger than in TM emission, since $|\mathbf{q}_\perp|$ in the former is much larger than in the latter (at a given emission angle). If the function $\phi_{-\mathbf{K}_{||}}(\mathbf{r}_\perp)$ lacks definite parity, then no selection rules can be imposed at all on LM transitions, as is obvious from Eqs. (59)—(61). Finally, even if we can ignore nondipolar effects caused by $q_\perp$ (this can be done at $|\hat{\mathbf{q}}_\perp|\ll 1/\gamma_i^2$, where $|q_\perp|\ll K_{||}$) and consider a definite parity of $\phi_{-\mathbf{K}_{||}}(\mathbf{r}_\perp)$, the selection rules are relaxed by the fact that $\mathbf{R}_{\rm if}^{(\mathbf{K})}$ always permits both odd and even $\{n_i\}-\{n_f\}$ values.

We proceed to analyze the angular dependence of the emission rate associated with a particular $\{n_i\}\to\{n_f\},\mathbf{K}$ transition, restricting ourselves to emission in the x-z plane, i.e., to $\phi=0$ (the polar axis directed along z).

(1) In the limit of small quantum recoil ($r_q\ll 1$), this angular dependence, as implied by Eq. (1), is given by

$$\omega(\theta)/c\,(1-\beta_{0z}\cos\theta)$$

multiplied by Eq. (14). The resulting expression for TM emission, obtained using Eq. (66), is

$$\frac{\omega(\theta)}{c\,(1-\beta_{0z}\cos\theta)}|\mathscr{M}_{\rm if}^{(\mathbf{K}_\perp)}(\mathbf{q})|_{\rm SI}^2=\frac{\omega(\theta)}{c\,(1-\beta_{0z}\cos\theta)}|(M_{\rm if}^{(\mathbf{K}_\perp)})_x|^2\times\left[\cos^2\theta+4\left[\frac{mc\gamma_i}{\hbar}\right]^2\left[\frac{\omega(\theta)}{c_q}\right]^2\frac{\sin^2\theta}{\left[\epsilon_\perp^{(i)}-\epsilon_\perp^{(f)}+\dfrac{\omega^2(\theta)}{c_q^2}\sin^2\theta\right]^2}(\beta_{iy}^2+\beta_{iz}^2\sin^2\theta)\right.$$
$$\left.-4\left[\frac{mc\gamma_i}{\hbar}\right]\left[\frac{\omega(\theta)}{c_q}\right]\frac{1}{\epsilon_\perp^{(i)}-\epsilon_\perp^{(f)}+\dfrac{\omega^2(\theta)}{c_q^2}\sin^2\theta}\sin^2\theta\cos\theta\beta_{iz}\right]\ . \quad (67)$$

Here, $\omega(\theta)$ is given in the optical range by Eq. (32) and either by Eq. (35) (if $1-n_q\gg r_q$) or by Eq. (47) (in the opposite limit) in the range $\omega\gtrsim\omega_p$. For low γ_i, the angular emission intensity distribution given by Eq. (67) is broad and complicated. For $\gamma_i\gg 1$, on the other hand, it is strongly concentrated within the relativistic forward cone $|\theta|\lesssim 1/\gamma_i$, owing to the factor $(1-\beta_{0z}\cos\theta)^{-1}$ multiplied by the Doppler upshift of $\omega(\theta)$. At small emission angles, neglecting $\omega^2\sin^2\theta/c_q^2$ compared to $\epsilon_\perp^{(i)}-\epsilon_\perp^{(f)}$ and retaining only the leading term in Eq. (47), Eq. (67) reduces approximately to

$$\frac{\hbar[\epsilon_\perp^{(i)}(\gamma_i)-\epsilon_\perp^{(f)}(\gamma_i)]}{2m\gamma_i c(1-\beta_{iz}\cos\theta-d_\omega)(1-\beta_{0z}\cos\theta)}|(M_{\rm if}^{(\mathbf{K}_\perp)})_x|^2\left[\cos^2\theta+\frac{\sin^2\theta}{(1-\beta_{iz}\cos\theta-d_\omega)^2}(\beta_{iy}^2+\beta_{iz}^2\sin^2\theta)-\frac{2\sin^2\theta\cos\theta}{1-\beta_{iz}\cos\theta-d_\omega}\beta_{iz}\right]\ . \quad (68)$$

It is seen that, in the case where β_{iy}^2 is comparable with β_{iz}^2 (which can occur in the SRG), the emission distribution about the z axis is broader than in the case $\beta_{iy}\simeq 0$ (which is compatible with the CGG).

The corresponding expressions for LM emission [obtained using Eqs. (59)—(61)] are

$$\frac{\omega(\theta)}{c\,(1-\beta_{0z}\cos\theta)}|\mathscr{M}_{\rm if}^{(\mathbf{K}_{||}\neq 0)}(\mathbf{q})|_{\rm SI}^2=\frac{\omega(\theta)}{c\,(1-\beta_{0z}\cos\theta)}(\cos^2\theta\,|(T_{\rm if}^{(\mathbf{K})})_x|^2+|(Q_{\rm if}^{(\mathbf{K})})_y+(R_{\rm if}^{(\mathbf{K})})_y|^2+\sin^2\theta\,|(Q_{\rm if}^{(\mathbf{K})})_z+(R_{\rm if}^{(\mathbf{K})})_z|^2$$
$$-\tfrac{1}{2}\sin 2\theta\{T_{\rm if}^{(\mathbf{K})}[(Q_{\rm if}^{(\mathbf{K})})_z+(R_{\rm if}^{(\mathbf{K})})_z]^*+{\rm c.c.}\})\quad (69a)$$

in the SRG, and

$$\frac{\omega(\theta)}{c(1-\beta_{0z}\cos\theta)}(\cos^2\theta(T_{\rm if}^{(\mathbf{K})})_x^2+(T_{\rm if}^{(\mathbf{K})})_y^2+\sin^2\theta\,|\,(Q_{\rm if}^{(\mathbf{K})})_z+(R_{\rm if}^{(\mathbf{K})})_z\,|^2-\tfrac{1}{2}\sin 2\theta\{(T_{\rm if}^{(\mathbf{K})})_x[(Q_{\rm if}^{(\mathbf{K})})_z+(R_{\rm if}^{(\mathbf{K})})_z]^*+\text{c.c.}\}) \tag{69b}$$

in the CGG. As seen from Eqs. (69), treatments ignoring $\mathbf{R}_{\rm if}^{(\mathbf{K})}$ (see above) substantially underestimate the LM emission rate (a) at large angles, particularly at $\theta\sim\pi/2$ (this angular region is important at nonrelativistic particle energies, when the directional distribution of the radiation is broad) and (b) within the forward cone, for relativistic particles in the SRG [because the $(R_{\rm if}^{(\mathbf{K})})_y$ contribution is then important], whenever

$$|R_{\rm if}^{(\mathbf{K})}|\gtrsim|T_{\rm if}^{(\mathbf{K})}|,|\mathbf{Q}_{\rm if}^{(\mathbf{K})}|\ .$$

(2) In the limit of *large quantum recoil* ($r_q\lesssim 1$), the expressions (67) and (69) must be modified for spin-$\frac{1}{2}$ particles by using Eq. (10) instead of Eq. (14). The angular-dependence expression [as obtained from Eqs. (1), (6), and (14)] is then

$$\frac{\omega(\theta)(1-r_q)}{c(1-\beta_{0z}\cos\theta)}\frac{[1+1/\gamma_i(1-r_q)]}{1+1/\gamma_i}\left[\left[1+\frac{r_q}{2(2-r_q)}\right]|\mathscr{M}_{\rm if}^{(\mathbf{K})}|_{\rm SI}^2+\frac{r_q^2}{2(2-r_q)^2}|M_{\rm if}^{(\mathbf{K})}|^2\right], \tag{70}$$

$\omega(\theta)$ being given by the lower branch of Eq. (39) [or, depending on the type of radiation, by one of the equations (44)–(46)]. It is seen that the term proportional to r_q^2, which arises in part from spin-photon coupling, assigns uniform weight to all Cartesian components of $\mathbf{M}_{\rm if}^{(\mathbf{K})}$. Consequently, the contribution of $(\mathbf{M}_{\rm if}^{(\mathbf{K})})_{||}$ [of $(M_{\rm if}^{(K)})_Z\hat{\mathbf{z}}$ in the CGG] to the emission at small θ becomes important in the large r_q limit, for TM as well as LM transitions [provided these θ are allowed—cf. Eq. (43)]. In particular, $(R_{\rm if}^{(\mathbf{K})})_z$ strongly contributes to LM emission in the CGG for $r_q\lesssim 1$.

The expressions obtained above for the angular dependence of TM emission [Eqs. (67), (68), and (70)] are equivalent to the ones derived in Ref. 1, except for the overall $1-r_q$ factor that has not been included in the latter [cf. Eq. (6)]. Here these expressions have been given in an explicit form that permits a detailed comparison with LM emission at a given angle θ.

The evaluation of the total emission rate at given ω and $\hat{\mathbf{q}}$ involves the summation of $|M_{\rm if}^{(\mathbf{K})}(\mathbf{q})|^2$ weighted by $P_iP_{\{n_f\}}^{(\mathbf{K})}$ [cf. Eqs. (1) and (25)]. The P_i are given, to a good approximation, by [cf. Eqs. (53) and (54)]

$$P_i=P_{\{n_i\}}\simeq\left|\frac{1}{A_{\rm cell}}\int_{\rm cell}d\mathbf{r}_\perp e^{-i\mathbf{k}_{i\perp}\cdot\mathbf{r}_\perp}w_i(\mathbf{r}_\perp)\right|^2$$
$$=|c_0^{\{n_i,\mathbf{k}_{i\perp}\}}|^2\ . \tag{71}$$

The significant P_i determine the $\{n_i\}$ bands contributing to LM *as well as* TM emission. For each such $\{n_i\}$, the value of $\Omega_{\rm if}^{(\mathbf{K})}$ associated with $\omega(\hat{\mathbf{q}})$ [cf. Eqs. (31) and (32)] determines the set of contributing $\{n_f,\mathbf{k}_{f\perp}\},\mathbf{K}$.

For LM emission in the CGG, a unique value of $\mathbf{K}_{||}=K_z\hat{\mathbf{z}}$ is associated with $\omega(\hat{\mathbf{q}})$ (since $\beta_{iz}cK_z$ is then the predominant term in $\Omega_{\rm if}^{(\mathbf{K})}$). In contrast, in the SRG one must allow for possible degeneracy among several $\mathbf{K}_{||}$, which contribute to the same $\Omega_{\rm if}^{(\mathbf{K})}$ if

$$\hat{\boldsymbol{\beta}}_{iy}\cdot\mathbf{K}_y+\hat{\boldsymbol{\beta}}_{iz}\cdot\mathbf{K}_z\simeq\hat{\boldsymbol{\beta}}_{iy}\cdot\mathbf{K}_y'+\hat{\boldsymbol{\beta}}_{iz}\cdot\mathbf{K}_z'\ . \tag{72}$$

Hence, in order to ensure that LM transitions in the SRG give rise to distinct spectral peaks, the near-degeneracy condition of Eq. (72) should be avoided as much as possible by choosing substantially different $|\hat{\boldsymbol{\beta}}_{iy}|,|\hat{\boldsymbol{\beta}}_{iz}|$ (e.g., $|\hat{\boldsymbol{\beta}}_{iy}|\lesssim 5|\hat{\boldsymbol{\beta}}_{iz}|$), so that the frequency of a spectral line associated with a low-index $\mathbf{K}_{||}$ will nearly coincide only with frequencies of lines pertaining to high-index $\mathbf{K}_{||}'$. The latter lines are, however, usually much weaker than the former, since the squared amplitude of $\phi_{-\mathbf{K}_{||}'}(\mathbf{r}_\perp)$ [cf. Eq. (63)] is much smaller than that of $\phi_{-\mathbf{K}_{||}}(\mathbf{r}_\perp)$ if $K_{||}'\gg K_{||}$ (Ref. 47), so that [cf. Eqs. (59)–(61)]

$$|\mathscr{M}_{\rm if}^{(\mathbf{K}_{||}'\neq\mathbf{0})}|^2\ll|\mathscr{M}_{\rm if}^{(\mathbf{K}_{||}\neq\mathbf{0})}|^2\ .$$

The near degeneracy between different $\mathbf{K}_{||}$'s can then be disregarded.

A single $\mathbf{K}_\perp$ commonly contributes to the emission at $\omega(\hat{\mathbf{q}})$, if $\Omega_{\rm if}^{(\mathbf{K})}$ strongly depends on $\mathbf{K}_\perp$ (e.g., in TM CB[6,21]). In contrast, LM or TM emission from channeled particles, whose $\Omega_{\rm if}$ is nearly independent of $\mathbf{K}_\perp$ (cf. Refs. 39 and 1, 6, and 9), contains contributions from all the $\mathbf{K}_\perp$ for which

$$P_{\{n_f\}}^{(\mathbf{K}_\perp)}=\left|\frac{1}{A_{\rm cell}}\int_{\rm cell}d\mathbf{r}_\perp e^{-i(\mathbf{k}_{i\perp}-\mathbf{q}_\perp-\mathbf{K}_\perp)}w_f(\mathbf{r}_\perp)\right|^2$$
$$=|c_0^{\{n_f,\mathbf{k}_{i\perp}-\mathbf{q}_\perp-\mathbf{K}_\perp\}}|^2 \tag{73}$$

are significant. When summing

$$P_{\{n_f\}}^{(\mathbf{K}_\perp)}|\mathscr{M}_{\rm if}^{(\mathbf{K}_{||}+\mathbf{K}_\perp)}|^2$$

over $\mathbf{K}_\perp$, to obtain the total LM emission rate, we must take account of the fact that $\mathbf{R}_{\rm if}^{(\mathbf{K})}$ depends on $\mathbf{K}_\perp$ in *all* dynamical regimes of the particle, whereas the other components of both TM and LM transition matrix elements may be nearly independent of $\mathbf{K}_\perp$, as in the channeling regime [this follows from the form of $w_{\{n\}}(\mathbf{r}_\perp)$ and $\epsilon_\perp^{\{n\}}$ in this regime[1,6,9]].

The observability (or detectability) of a spectral peak at one of the frequencies discussed here depends on its "signal-to-noise" ratio (S/N)(ω), namely, the ratio of its emission rate to that of incoherent bremsstrahlung $dW_{inc}(\omega)$. Since $dW_{inc}(\omega)\propto\omega^{-1}$ (Refs. 4 and 6), from Eqs. (1) and (14) we find (assuming $r_q\ll 1$)

$$\frac{(S/N)(\omega_{LM},\hat{\mathbf{q}})}{(S/N)(\omega_{TM},\hat{\mathbf{q}})}=\left[\frac{\omega_{LM}}{\omega_{TM}}\right]\frac{dW(\omega_{LM},\hat{\mathbf{q}})}{dW(\omega_{TM},\hat{\mathbf{q}})}$$
$$=\left[\frac{\omega_{LM}}{\omega_{TM}}\right]^2\frac{\sum_i\sum_{f,\mathbf{K}}P_iP_f^{(\mathbf{K})}|\mathscr{M}_{if}^{(\mathbf{K}_{||}\neq 0)}|^2}{\sum_i\sum_{f,\mathbf{K}_\perp}P_iP_f^{(\mathbf{K}_\perp)}|\mathscr{M}_{if}^{(\mathbf{K}_\perp)}|^2}\ . \tag{74}$$

The ratio given by Eq. (74) is also the ratio between the amounts of power emitted in the two modes in the same direction:

$$\frac{I(\omega_{LM},\hat{\mathbf{q}})}{I(\omega_{TM},\hat{\mathbf{q}})}=\left[\frac{\hbar\omega_{LM}}{\hbar\omega_{TM}}\right]\frac{dW(\omega_{LM},\hat{\mathbf{q}})}{dW(\omega_{TM},\hat{\mathbf{q}})}=\frac{(S/N)(\omega_{LM},\hat{\mathbf{q}})}{(S/N)(\omega_{TM},\hat{\mathbf{q}})}\ . \tag{75}$$

Our classical analysis of LM and TM emission from channeled positrons in the CGG (Ref. 25) has shown that this ratio can be ~ 1. As seen from Eq. (1), $\hbar\omega dW$ does not depend explicitly on $\hbar$. Hence, this classical result, which implies that LM emission is as detectable as TM emission, may be expected to hold quantum mechanically too. However, it is planned to be shown in subsequent papers that, in certain cases, LM emission is more intense than what is predicted classically and as a result is then more detectable than TM emission. This finding is in accordance with recent experimental results.[29]

V. DISCUSSION

In this paper we have presented a unified quantal treatment of all types of radiation (CR, TM CB, QCR, PR, and LM emission—cf. Sec. I) emitted as fast charged particles traverse crystals at small angles relative to atomic rows (the CGG) or planes (the SRG). This treatment consists in the description of the entire spectrum of this radiation by formulas that allow for the full three-dimensional periodicity of the crystal potential and are applicable to energies of all photons [cf. Eqs. (1), (6), (10), and (39)]. These include photon energies comparable to the initial particle energy, a case that has been insufficiently studied hitherto, although it is realizable experimentally. The formulas presented here take account of the essential feature of the investigated radiation, namely, the possibility of momentum transfer $\hbar\mathbf{K}$ to the lattice in all three dimensions (LM emission—if $\mathbf{K}$ has a longitudinal component, TM emission if $\mathbf{K}$ is purely transverse) in conjunction with transitions between bands of transverse energy [cf. Eqs. (10), (23), and (32)]. The generality of these formulas allows us to use them in a systematic, comprehensive analysis of the emission spectrum, as a function of the parameters of the incident particle and the direction of emission.

In the following we survey the main topics elucidated by the present treatment.

(A) Our analysis of the allowed *emission frequencies* has yielded expressions that are valid for all types of TM and LM radiative transitions in (1) the optical range, with the refractivity index exceeding 1; (2) the range $\omega>\omega_p$ (ω_p being the plasma frequency of the medium), with the refractivity index given by Eq. (34); and (3) the range where the quantum recoil $r_q=\hbar\omega/E_i$ (E_i being the initial particle energy) becomes appreciable. In case (2) we have discussed the forbidden emission angles for TM transitions due to refractivity effects [Eq. (36)] and the shifts of LM and TM frequencies caused by these effects [Eqs. (35) and (37)]. In case (3) (Sec. III C) the large-quantum-recoil limit ($r_q\lesssim 1$) has been shown to correspond to nearly forward emission at frequencies that differ strongly from those obtained in the more familiar small-recoil limit. Forbidden emission angles for LM and TM CB transitions, associated with photon energies above the initial kinetic energy of the particle, have been identified [Eqs. (43) and (46)]. In the limit $r_q\ll 1$, our analysis has revealed quantum-recoil corrections [Eqs. (47)—(49)] to the frequencies given by extant theories.

(B) Expressions for spectral linewidths incurred by inelastic scattering of the particle [Eqs. (26) and (27)] or finite crystal thickness [Eq. (29)] have been presented in a form appropriate for all types of radiative transitions and any quantum recoil [Eqs. (52)] (whereas the previous extensive investigation of this problem[50] has concentrated on CR in the limit $r_q\ll 1$).

(C) LM transition matrix elements have been found to include a significant component (the *leading component* in some cases) $\mathbf{R}_{if}^{(\mathbf{K})}$, which is proportional to the longitudinal velocity $\boldsymbol{\beta}_{i||}$ [Eq. (61)]. This component has not been taken into account in a previous analysis of LM emission from channeled particles,[28] nor can it be obtained using an extant treatment of longitudinal potential periodicity effects.[40] The existence of $\mathbf{R}_{if}^{(\mathbf{K})}$ has been shown to relax the selection rules on the allowed differences between initial and final band indices $\{n_i\}-\{n_f\}$ in LM emission.

(D) Expressions allowing comparison of the directional distribution of TM emission with that of LM emission have been derived, for the small-recoil limit $r_q\ll 1$ [Eqs. (67)—(69)] as well as for the large-recoil limit $r_q\lesssim 1$. In the latter, spin-photon coupling can strongly affect the directional distribution of emission from spin-$\frac{1}{2}$ particles [Eq. (70)]. In both limits, it has been shown that the LM emission rate in certain directions $\hat{\mathbf{q}}$ may be severely underestimated if $\mathbf{R}_{if}^{(\mathbf{K})}$ is not taken into account.

(E) An expression for the relative detectabilities of LM and TM spectral lines (determined by the ratios of their respective emission rates to that of incoherent bremsstrahlung) has been given [Eq. (74)]. This expression, which coincides with the ratio

$$[dI(\omega_{LM},\hat{\mathbf{q}})/d\Omega_{\hat{\mathbf{q}}}]/[dI(\omega_{TM},\hat{\mathbf{q}})/d\Omega_{\hat{\mathbf{q}}}]$$

($dI/d\Omega_{\hat{\mathbf{q}}}$ being the differential emitted power), has been previously shown classically to be ~ 1 for channeled positrons.[25]

In subsequent parts of this series, the present treatment will be used to investigate, for each of the aforementioned types of radiation, spectral features imposed by the transverse or the longitudinal potential periodicity which are not describable analytically by the prevailing models. These investigations will concentrate on particles in the SRG. For such particles, analytical forms of the project-

ed potential eigenfunctions and eigenvalues (transverse-energy bands), which constitute the required input for both TM and LM emission calculations (cf. Sec. IV and the Appendix), can be obtained using the Hill's equation treatment presented in Ref. 39. In contrast, the standard many-beam treatment[7,8,14,47] and the KKR treatment (appropriate in the CGG, Ref. 67) can yield this input only numerically for β particles above 10 MeV and all heavy fast particles.

ACKNOWLEDGMENTS

We are indebted to Professor M. O. Scully for his continuous interest, encouragement, and support. One of us (G.K.) is grateful to Professor J. U. Andersen, Professor S. Datz, and Professor B. L. Berman for stimulating discussions. Parts of this work are based on the Ph.D. dissertation of G.K. (University of New Mexico, 1983). This work was supported in part by the U.S. Office of Naval Research, Department of the Navy.

APPENDIX: EVALUATION OF LM TRANSITION MATRIX ELEMENTS

The evaluation of LM transition matrix elements requires explicit expressions for the longitudinal-modulation terms

$$\exp(i\mathbf{h}_{||}\cdot\mathbf{r}_{||})\delta w_{\{n\mathbf{k}_\perp\}}^{(\mathbf{h}_{||})}(\mathbf{r}_\perp)$$

[cf. Eqs. (53) and (57)] or their Fourier coefficients $c_{\mathbf{h}=\mathbf{g}_\perp+\mathbf{g}_{||}}$. Such expressions are derived in Ref. 39, using an iterative procedure which yields, on performing two iterations,

$$\begin{aligned} c_{\mathbf{h}}^{\{n,\mathbf{k}_\perp\}} = &-\chi_{\mathbf{h}_{||}}\sum_{\mathbf{g}'_\perp}\phi_{\mathbf{h}-\mathbf{g}'_\perp}(c_{\mathbf{g}'_\perp}^{\{n,\mathbf{k}_\perp\}}+\delta c_{\mathbf{g}'_\perp}^{\{n,\mathbf{k}_\perp\}}) \\ &-\chi_{\mathbf{h}_{||}}\kappa_{\mathbf{h}}^{\{n,\mathbf{k}_\perp\}}\sum_{\mathbf{g}'_\perp}\phi_{\mathbf{h}-\mathbf{g}'_\perp}c_{\mathbf{g}'_\perp}^{\{n,\mathbf{k}_\perp\}} \\ &+\chi_{\mathbf{h}_{||}}\sum_{\substack{\mathbf{h}' \\ (\mathbf{h}'_{||}\neq 0)}}\chi_{\mathbf{h}'_{||}}\phi_{\mathbf{h}-\mathbf{h}'}\sum_{\mathbf{g}'_\perp}\phi_{\mathbf{h}-\mathbf{g}'_\perp}c_{\mathbf{g}'_\perp}^{\{n,\mathbf{k}_\perp\}} \\ &+O(\chi_{h_{||}}^2\kappa_h,\chi_{h_{||}}^3,\chi_{h_{||}}\kappa_h^2)\ . \end{aligned} \tag{A1}$$

Here the ϕ's and χ's are defined in Eqs. (63) and (64). The factor $\kappa_{\mathbf{h}}^{\{n,\mathbf{k}_\perp\}}$ is given by

$$\kappa_{\mathbf{h}}^{\{n,\mathbf{k}_\perp\}}\simeq\frac{1}{2\mathbf{k}_{0||}\cdot\mathbf{h}_{||}}\left[\frac{h_{||}\epsilon_\perp^{\{n,\mathbf{k}_\perp\}}}{k_{0||}}+\epsilon_\perp^{\{n,\mathbf{k}_\perp\}}-(\mathbf{k}_\perp+\mathbf{h})^2\right], \tag{A2}$$

and typically satisfies $|\kappa_{\mathbf{h}}^{\{n,\mathbf{k}_\perp\}}|\gtrsim|\chi_{\mathbf{h}_{||}}|$. The corrections $\delta c_{\mathbf{g}'_\perp}^{\{n,\mathbf{k}_\perp\}}$ to the transverse Fourier coefficients $c_{\mathbf{g}'_\perp}^{\{n,\mathbf{k}_\perp\}}$ of the projected potential eigenfunctions are found from

$$[\tilde{\epsilon}_\perp^{\{n,\mathbf{k}_\perp\}}-(\mathbf{k}_\perp+\mathbf{g}_\perp)^2](\delta c_{\mathbf{g}_\perp}^{\{n,\mathbf{k}_\perp\}}+c_{\mathbf{g}_\perp}^{\{n,\mathbf{k}_\perp\}})=\sum_{\mathbf{g}'_\perp(\neq 0)}\left[U_{\mathbf{g}'_\perp}-\sum_{\mathbf{h}(\neq 0)}\chi_{\mathbf{h}}\sum_{\mathbf{g}''_\perp}\phi_{\mathbf{g}'_\perp+\mathbf{g}''_\perp-\mathbf{h}}U_{\mathbf{h}-\mathbf{g}''_\perp}\right](\delta c_{\mathbf{g}_\perp-\mathbf{g}'_\perp}^{\{n,\mathbf{k}_\perp\}}+c_{\mathbf{g}_\perp-\mathbf{g}'_\perp}^{\{n,\mathbf{k}_\perp\}})+O(\chi_{\mathbf{h}}^2,\chi_{\mathbf{h}}\kappa_{\mathbf{h}})\ , \tag{A3}$$

where $\tilde{\epsilon}_\perp^{\{n,\mathbf{k}_\perp\}}$ are transverse-energy eigenvalues corrected for the longitudinal variation of the potential.

The terms comprising the LM transition matrix element $\mathbf{M}_{\mathrm{if}}^{(\mathbf{K}_{||}\neq 0)}(\mathbf{q})$ in Eq. (58) originate from its decomposition into transverse and longitudinal components, on using Eq. (23) and setting

$$\mathbf{T}_{\mathrm{if}}^{(\mathbf{K})}=(\mathbf{M}_{\mathrm{if}}^{(\mathbf{K})})_\perp=\sum_{\mathbf{g}}[\beta_{i\perp}c_{\mathbf{g}}^{(i)}(c_{\mathbf{g}+\mathbf{K}}^{(f)})^*+\beta_{\mathbf{g}_\perp}c_{\mathbf{g}}^{(i)}(c_{\mathbf{g}+\mathbf{K}}^{(f)})^*]\ , \tag{A4}$$

$$\mathbf{Q}_{\mathrm{if}}^{(\mathbf{K})}=\sum_{\mathbf{g}}\beta_{\mathbf{g}_{||}}c_{\mathbf{g}}^{(i)}(c_{\mathbf{g}+\mathbf{K}}^{(f)})^*\ , \tag{A5}$$

$$\mathbf{R}_{\mathrm{if}}^{(\mathbf{K})}=\beta_{i||}\sum_{\mathbf{g}}c_{\mathbf{g}}^{(i)}(c_{\mathbf{g}+\mathbf{K}}^{(f)})^*\ . \tag{A6}$$

To the lowest admissible accuracy, $\mathbf{T}_{\mathrm{if}}^{(\mathbf{K})}$ and $\mathbf{Q}_{\mathrm{if}}^{(\mathbf{K})}$ include only contributions of order $|\chi_{K_{||}}|$ from the expansion given by Eq. (A1):

$$\mathbf{T}_{\mathrm{if}}^{(\mathbf{K})}=-\chi_{\mathbf{K}_{||}}\sum_{\mathbf{g}_\perp}\sum_{\mathbf{g}'_\perp}(\beta_{\mathbf{g}'_\perp}-\beta_{\mathbf{g}_\perp}-\beta_{\mathbf{K}_\perp})[\phi_{\mathbf{g}'_\perp-\mathbf{g}_\perp-\mathbf{K}}c_{\mathbf{g}_\perp}^{(i)}(c_{\mathbf{g}'_\perp}^{(f)})^*+O(\kappa_{\mathbf{g}},\chi_{\mathbf{g}_{||}})]\ , \tag{A7}$$

$$\mathbf{Q}_{\mathrm{if}}^{(\mathbf{K})}=-\chi_{\mathbf{K}_{||}}\beta_{\mathbf{K}_{||}}\sum_{\mathbf{g}_\perp}\sum_{\mathbf{g}'_\perp\neq 0}[\phi_{\mathbf{g}'_\perp-\mathbf{g}_\perp-\mathbf{K}}c_{\mathbf{g}_\perp}^{(i)}(c_{\mathbf{g}'_\perp}^{(f)})^*+O(\kappa_{\mathbf{g}},\chi_{\mathbf{g}_{||}})]\ . \tag{A8}$$

To the *same accuracy*, one must take account of contributions of order $|\chi_{\mathbf{K}_{||}}\kappa_{\mathbf{g}}|, |\chi_{\mathbf{K}_{||}}\chi_{\mathbf{h}_{||}}|$ to $\mathbf{R}_{\mathrm{if}}^{(\mathbf{K})}$ (the contributions of order $|\chi_{\mathbf{K}_{||}}|$ to $\mathbf{R}_{\mathrm{if}}^{(\mathbf{K})}$ can be easily shown *to vanish*), because typically

$$|\beta_{\mathbf{g}}|, |\beta_{i\perp}|\lesssim|\beta_{i||}\chi_{\mathbf{h}_{||}}|, |\beta_{i||}\kappa_{\mathbf{g}}|\ . \tag{A9}$$

The lengthy but straightforward evaluation of $\mathbf{R}_{\mathrm{if}}^{(\mathbf{K})}$, taking account of the above contributions, shows that the sum of all $\delta c_{\mathbf{g}_\perp}^{(\mathbf{K})}$ contributions is

$$\sum_{\mathbf{g}_\perp}\sum_{\mathbf{g}'_\perp}[\phi_{\mathbf{g}'_\perp-\mathbf{g}_\perp-\mathbf{K}}\delta c_{\mathbf{g}_\perp}^{(i)}(c_{\mathbf{g}'_\perp}^{(f)})^*-\phi_{\mathbf{g}_\perp-\mathbf{g}'_\perp-\mathbf{K}}\delta c_{\mathbf{g}'_\perp}^{(i)}(c_{\mathbf{g}_\perp}^{(f)})^*]=0\ . \tag{A10}$$

The remaining contributions to $\mathbf{R}_{\mathrm{if}}^{(\mathbf{K})}$ yield

$$\mathbf{R}_{if}^{(\mathbf{K})}=\boldsymbol{\beta}_{i\parallel}\left[\chi_{\mathbf{K}_\parallel}\sum_{\mathbf{g}_\perp}\sum_{\mathbf{g}'_\perp}\kappa^{(\mathbf{K})}_{\mathbf{g}_\perp,\mathbf{g}'_\perp}\phi_{\mathbf{g}'_\perp-\mathbf{g}_\perp-\mathbf{K}}c^{(i)}_{\mathbf{g}_\perp}(c^{(f)}_{\mathbf{g}'_\perp})^*\right.$$
$$\left.+\sum_{\substack{\mathbf{g}\\(\mathbf{g}_\parallel\neq 0)}}\chi_{\mathbf{K}_\parallel+\mathbf{g}_\parallel}\chi_{\mathbf{g}_\parallel}\left[\sum_{\mathbf{g}'_\perp}\sum_{\mathbf{g}''_\perp}[\phi_{\mathbf{g}_\perp-\mathbf{g}'_\perp+\mathbf{g}_\parallel}c^{(i)}_{\mathbf{g}'_\perp}(c^{(f)}_{\mathbf{g}''_\perp})^*+\phi_{\mathbf{g}''_\perp-\mathbf{g}_\perp-\mathbf{K}_\perp-(\mathbf{g}_\parallel+\mathbf{K}_\parallel)}]\right]\right]+O(\chi^3_{\mathbf{h}_\parallel},\chi_{\mathbf{h}_\parallel}\kappa_{\mathbf{h}})\ . \tag{A11}$$

The factors $\kappa^{(\mathbf{K})}_{\mathbf{g}_\perp,\mathbf{g}'_\perp}$ are derived from the expressions for $(\kappa^{(f)}_{\mathbf{g}'_\perp+\mathbf{K}})^*$ and $\kappa^{(i)}_{\mathbf{g}_\perp-\mathbf{K}}$ [cf. Eq. (A2)]. They have the form

$$\kappa^{(\mathbf{K})}_{\mathbf{g}_\perp,\mathbf{g}'_\perp}=-\frac{\hbar(\epsilon^{(i)}_\perp+\epsilon^{(f)}_\perp-k^2_{i\perp}-k^2_{f\perp})}{2mc\gamma_i\boldsymbol{\beta}_{i\parallel}\cdot\mathbf{K}_\parallel}+\frac{\mathbf{K}_\perp}{\boldsymbol{\beta}_{i\parallel}\cdot\mathbf{K}_\parallel}\cdot(\boldsymbol{\beta}_{f\perp}-\boldsymbol{\beta}_{i\perp})+\frac{\boldsymbol{\beta}_\mathbf{K}\cdot\mathbf{K}}{\boldsymbol{\beta}_{i\parallel}\cdot\mathbf{K}}$$
$$+\frac{\mathbf{g}_\perp}{\boldsymbol{\beta}_{i\parallel}\cdot\mathbf{K}_\parallel}\cdot\left[\frac{\boldsymbol{\beta}_{i\perp}+\boldsymbol{\beta}_{\mathbf{g}_\perp}}{2}+(\boldsymbol{\beta}_{i\parallel}\cdot\boldsymbol{\beta}_{\mathbf{K}_\parallel})\hat{\mathbf{q}}_\perp/(1-\boldsymbol{\beta}_{i\parallel}\cdot\hat{\mathbf{q}}_\parallel)\right]+\frac{\mathbf{g}'_\perp}{\boldsymbol{\beta}_{i\parallel}\cdot\mathbf{K}_\parallel}\cdot\left[\boldsymbol{\beta}_{\mathbf{K}_\perp}+\frac{\boldsymbol{\beta}_{i\perp}+\boldsymbol{\beta}_{\mathbf{g}_\perp}}{2}\right], \tag{A12}$$

where $\mathbf{k}_{f\perp}$ is found from Eq. (50) on using the first-iteration value of $\omega\hat{\mathbf{q}}/c$ [cf. discussion following Eq. (50)].

The above expressions for the components of the LM transition matrix element can be evaluated using the $c_{\mathbf{g}_\perp}$ coefficients of the projected-potential eigenfunctions, which are available either analytically or numerically. These expressions assume a more transparent form in the coordinate representation. The transformation to this representation is effected using the following identities:

$$\sum_{\mathbf{g}_\perp}\sum_{\mathbf{g}'_\perp}\phi_{\mathbf{g}'_\perp-\mathbf{g}_\perp-\mathbf{K}}c^{(i)}_{\mathbf{g}_\perp}(c^{(f)}_{\mathbf{g}'_\perp})^*=\int_{\text{cell}}d\mathbf{r}_\perp e^{-i\mathbf{q}_\perp\cdot\mathbf{r}_\perp}\phi_{-\mathbf{K}_\parallel}(\mathbf{r}_\perp)[w^{(f)}(\mathbf{r}_\perp)]^*w^{(i)}(\mathbf{r}_\perp)\ , \tag{A13}$$

$$i\sum_{\mathbf{g}_\perp}\sum_{\mathbf{g}'_\perp}(\mathbf{k}_{i\perp}+\mathbf{g}_\perp)\phi_{\mathbf{g}'_\perp-\mathbf{g}_\perp-\mathbf{K}}c^{(i)}_{\mathbf{g}_\perp}(c^{(f)}_{\mathbf{g}'_\perp})^*=\int_{\text{cell}}d\mathbf{r}_\perp e^{-i\mathbf{q}_\perp\cdot\mathbf{r}_\perp}\phi_{-\mathbf{K}_\parallel}(\mathbf{r}_\perp)[w^{(f)}(\mathbf{r}_\perp)]^*\nabla_\perp w^{(i)}(\mathbf{r}_\perp)\ , \tag{A14}$$

$$-i\sum_{\mathbf{g}_\perp}\sum_{\mathbf{g}'_\perp}(\mathbf{k}_{f\perp}+\mathbf{g}'_\perp)\phi_{\mathbf{g}'_\perp-\mathbf{g}_\perp-\mathbf{K}}c^{(i)}_{\mathbf{g}_\perp}(c^{(f)}_{\mathbf{g}'_\perp})^*=\int_{\text{cell}}d\mathbf{r}_\perp e^{-i\mathbf{q}_\perp\cdot\mathbf{r}_\perp}\phi_{-\mathbf{K}_\parallel}(\mathbf{r}_\perp)\{\nabla_\perp[w^{(f)}(\mathbf{r}_\perp)]^*\}w^{(i)}(\mathbf{r}_\perp)\ , \tag{A15}$$

$$-\sum_{\mathbf{g}_\perp}\sum_{\mathbf{g}'_\perp}(\mathbf{k}_{i\perp}+\mathbf{g}_\perp)^2\phi_{\mathbf{g}'_\perp-\mathbf{g}_\perp-\mathbf{K}}c^{(i)}_{\mathbf{g}_\perp}(c^{(f)}_{\mathbf{g}'_\perp})^*=\int_{\text{cell}}d\mathbf{r}_\perp e^{-i\mathbf{q}_\perp\cdot\mathbf{r}_\perp}\phi_{-\mathbf{K}_\parallel}(\mathbf{r}_\perp)w^{*(f)}(\mathbf{r}_\perp)\nabla^2_\perp w(\mathbf{r}_\perp)\ , \tag{A16}$$

$$\sum_{\mathbf{g}_\perp}\sum_{\mathbf{g}'_\perp}(\mathbf{g}_\perp\cdot\mathbf{g}'_\perp)\phi_{\mathbf{g}'_\perp-\mathbf{g}_\perp-\mathbf{K}}c^{(i)}_{\mathbf{g}_\perp}(c^{(f)}_{\mathbf{g}'_\perp})^*$$
$$=\int_{\text{cell}}d\mathbf{r}_\perp e^{-i\mathbf{q}_\perp\cdot\mathbf{r}_\perp}\phi_{-\mathbf{K}_\parallel}(\mathbf{r}_\perp)\{[\nabla_\perp(w^{(f)})^*]\cdot(\nabla_\perp w^{(i)})+i\mathbf{k}_{f\perp}\cdot[(w^{(f)})^*\nabla_\perp w^{(i)}]-i\mathbf{k}_{i\perp}\cdot[\nabla_\perp(w^{(f)})^*]w^{(i)}+\mathbf{k}_{i\perp}\cdot\mathbf{k}_{f\perp}(w^{(f)})^*w^{(i)}\}\ , \tag{A17}$$

$$\sum_{\substack{\mathbf{g}\\(\mathbf{g}_\parallel\neq 0)}}\sum_{\mathbf{g}'_\perp}\sum_{\mathbf{g}''_\perp}[\chi_{\mathbf{K}_\parallel+\mathbf{g}_\parallel}\chi_{\mathbf{g}_\parallel}c^{(i)}_{\mathbf{g}'_\perp}(c^{(f)}_{\mathbf{g}''_\perp})^*\phi_{\mathbf{g}_\perp-\mathbf{g}'_\perp+\mathbf{g}_\parallel}\phi_{\mathbf{g}''_\perp-\mathbf{g}_\perp-\mathbf{K}-(\mathbf{g}_\parallel+\mathbf{K}_\parallel)}]$$
$$=\sum_{\mathbf{g}_\parallel}\chi_{\mathbf{K}_\parallel+\mathbf{g}_\parallel}\chi_{\mathbf{g}_\parallel}\int_{\text{cell}}d\mathbf{r}_\perp e^{-i\mathbf{q}_\perp\cdot\mathbf{r}_\perp}\phi_{\mathbf{g}_\parallel}(\mathbf{r}_\perp)\phi_{-(\mathbf{g}_\parallel+\mathbf{K}_\parallel)}(\mathbf{r}_\perp)[w^{(f)}(\mathbf{r}_\perp)]^*w^{(i)}(\mathbf{r}_\perp)\ . \tag{A18}$$

The expressions (A7), (A8), and (A11) can be easily transformed into Eqs. (59)—(61) by using the above identities.

[1]V. V. Beloshitsky and F. F. Komarov, Phys. Rep. **93**, 117 (1982), and references therein.

[2]N. P. Kalashnikov and N. N. Strikhanov, Kvantovaya Elektron. (Moscow) **8**, 2293 (1981) [Sov. J. Quantum Electron. **11**, 1405 (1981)], and references therein.

[3]V. A. Bazylev and N. K. Zhevago, Radiat. Eff. **54**, 41 (1981).

[4]R. Wedell, Phys. Status Solidi B **99**, 11 (1980).

[5]J. U. Andersen and E. Bonderup, in *Annual Review of Nuclear Particle Science*, edited by J. B. Jackson, H. E. Gove, and R. Y. Schwitters (Annual Reviews, Palo Alto, 1983), p. 453.

[6]J. U. Andersen, K. R. Eriksen, and E. Laegsgaard, Phys. Scr. **24**, 588 (1981).

[7]S. Datz, R. W. Fearick, H. Park, R. H. Pantell, R. L. Swent, J. O. Kephart, and B. L. Berman, Nucl. Instrum. Methods **B2**, 74 (1984).

[8]R. L. Swent, R. H. Pantell, M. J. Alguard, B. L. Berman, S. D. Bloom, and S. Datz, Phys. Rev. Lett. **43**, 1723 (1979).

[9]D. M. Bird and B. F. Buxton, Proc. R. Soc. London, Ser. A **379**, 459 (1982).

[10]M. A. Kumakhov, Zh. Eksp. Teor. Fiz. **72**, 1489 (1977) [Sov. Phys.—JETP **45**, 781 (1977)].

[11]M. A. Kumakhov, Phys. Status Solidi B **84**, 41 (1977).

[12]M. A. Kumakhov and R. Wedell, Phys. Status Solidi B **84**, 581 (1977).

[13]R. H Pantell and M. J. Alguard, J. Appl. Phys. **50**, 798 (1979).
[14]A. V. Tulupov, Radiat. Eff. **62**, 77 (1982).
[15]A. L. Avakian, N. K. Zhevago, and Yan Shi, Zh. Eksp. Teor. Fiz. **82**, 573 (1982) [Sov. Phys.—JETP **55**, 341 (1982)]; V. A. Bazylev and A. V. Demura, Radiat. Eff. **61**, 129 (1982).
[16]A. V. Andreev, S. A. Akhmanov, V. A. Vysloukh, and V. L. Kuznetsov, Zh. Eksp. Teor. Fiz. **84**, 1743 (1983) [Sov. Phys.—JETP **57**, 1017 (1983).
[17]H. Überall, Phys. Rev. **103**, 1055 (1956).
[18]G. Diambrini-Palazzi, Rev. Mod. Phys. **40**, 611 (1968).
[19]H. Mendlowitz and S. J. Glass, Opt. Commun. **41**, 37 (1982).
[20]M. L. Ter-Mikaelian, *High-Energy Electromagnetic Processes in Condensed Media* (Wiley-Interscience, New York, 1972); A. I. Akhiezer, Fiz. Elem. Chastits At. Yadra **10**, 51 (1979) [Sov. J. Part. Nucl. **10**, 19 (1979)].
[21]I. A. Grishaev, G. D. Kovalenko, and B. I. Shramenko, Zh. Eksp. Teor. Fiz. **72**, 437 (1977) [Sov. Phys.—JETP **45**, 229 (1977)].
[22]R. L. Walker, B. L. Berman, and S. D. Bloom, Phys. Rev. A **11**, 736 (1975).
[23]V. V. Fedorov and A. I. Smirnov, Zh. Eksp. Teor. Fiz. **66**, 566 (1974) [Sov. Phys.—JETP **39**, 271 (1974)].
[24]J. C. H. Spence and C. J. Humphreys, Optik (Stuttgart) **66**, 225 (1984).
[25]G. Kurizki and J. K. McIver, Phys. Lett. **89A**, 43 (1982).
[26]A. W. Saenz and H. Überall, Phys. Rev. B **25**, 4418 (1982).
[27]H. Überall and A. W. Saenz, Phys. Lett. **90A**, 370 (1982).
[28]R. V. Vedrinskii and V. S. Malyshevskii, Zh. Eksp. Teor. Fiz. **83**, 899 (1982) [Sov. Phys.—JETP **56**, 506 (1982)].
[29]J. C. H. Spence, G. Reese, N. Yamamoto, and G. Kurizki, Philos. Mag. **B48**, L39 (1983).
[30]G. M. Reese, J. C. H. Spence, and N. Yamamoto, Philos. Mag. **A49**, 697 (1984).
[31]G. Kurizki and J. K. McIver, in *LASERS'82 International Conference Proceedings*, edited by R. C. Powell (STS Press, McLean, Virginia, 1984).
[32]G. Kurizki and J. K. McIver, Nucl. Instrum. Methods **B2**, 67 (1984).
[33]Yu. N. Adishchev, A. N. Didenko, V. N. Zabaev, B. N. Kalinin, A. A. Kurkov, A. P. Potylitsin, V. K. Tomchakov, and A. S. Vorobiev, Radiat. Eff. **60**, 61 (1982).
[34]M. V. Berry, B. F. Buxton, and A. M. Ozorio de Almeida, Radiat. Eff. **20**, 1 (1973).
[35]M. V. Berry, J. Phys. C **4**, 697 (1971).
[36]P. Lervig, J. Lindhard, and V. Nielsen, Nucl. Phys. A **96**, 481 (1967).
[37]J. Lindhard, K. Dan. Vidensk. Selsk. Mat. Fys. Medd. **34**, No. 14 (1965).
[38]D. S. Gemmell, Rev. Mod. Phys. **46**, 129 (1974).
[39]G. Kurizki, Phys. Rev. B (to be published).
[40]B. F. Buxton, Proc. R. Soc. London, Ser. A **350**, 335 (1976).
[41]V. B. Berestetskii, E. M. Lifshitz, and L. P. Pitaevskii, *Relativistic Quantum Theory* (Pergamon, Oxford, 1971), part 1.
[42]R. P. Feynman, *Quantum Electrodynamics* (Benjamin, Reading, Mass., 1962).
[43]V. G. Baryshevskii, A. O. Grubich, and I. Ya. Dubovskaya, Phys. Status Solidi B **88**, 351 (1978).
[44]U. Fano, H. W. Koch, and J. W. Motz, Phys. Rev. **112**, 1679 (1958).
[45]K. Fujiwara, J. Phys. Soc. Jpn. **17**, 2226 (1961).
[46]V. Weisskopf, Z. Phys. **93**, 561 (1935).
[47]P. B. Hirsch, A. Howie, R. B. Nicholson, D. W. Pashley, and M. J. Whelan, *Electron Microscopy of Thin Crystals* (Butterworth, London, 1965).
[48]A. Howie, Philos. Mag. **14**, 223 (1966).
[49]J. M. Cowley, *Diffraction Physics* (North-Holland, Amsterdam, 1981).
[50]*Electron Diffraction* 1927-1977, edited by P. J. Dobson, J. B. Pendry, and D. J. Humphreys (IOP, London, 1978).
[51]S. V. Plotnikov, D. E. Popov, E. I. Rozum, O. G. Kostareva, and S. A. Vorobiev, Phys. Status Solidi **103B**, 81 (1981).
[52]K. Kambe, G. Lehmpfuhl, and F. Fujimoto, Z. Naturforsch. **29A**, 1034 (1974).
[53]Effects of the longitudinal variation of the potential on the diffraction pattern of the particle have been studied (before Ref. 39) by B. F. Buxton, Proc. R. Soc. London, Ser. A. **350**, 335 (1976). See the criticism of the latter approach in Ref. 39.
[54]The association of LM emission with longitudinal Fourier coefficients of the Bloch waves has been first proposed in Ref. 31 [other works related to LM emission (Refs. 25–30 and 32) are surveyed in Sec. I].
[55]P. A. Doyle and P. S. Turner, Acta Crystallogr. **A24**, 390 (1968).
[56]A. Howie and R. M. Stern, Z. Naturforsch. **27A**, 382 (1972); D. Cherns, A. Howie, and M. H. Jacobs, Z. Naturforsch. **28A**, 565 (1973).
[57]P. M. Dederichs, Solid State Phys. **27**, 135 (1972).
[58]J. U. Andersen, E. Bonderup, E. Laegsgaard, and A. H. Sørensen, Phys. Scr. **28**, 308 (1983).
[59]M. J. Whelan, J. Appl. Phys. **36**, 2099 (1965).
[60]M. J. Whelan, J. Appl. Phys. **36**, 2103 (1965).
[61]V. V. Beloshitsky, Phys. Lett. **64A**, 95 (1977).
[62]V. G. Baryshevskii, I. Ya. Dubovskaya, and O. T. Gradovsky, Phys. Lett. **91A**, 135 (1982).
[63]V. A. Bazylev and N. K. Zhevago, Usp. Fiz. Nauk **127**, 529 (1979) [Sov. Phys.—Usp. **22**, 191 (1979)]; Zh. Eksp. Teor. Fiz. **73**, 1684 (1977) [Sov. Phys.—JETP **46**, 894 (1977)].
[64]V. G. Baryshevskii and I. Ya. Dubovskaya, Dokl. Akad. Nauk SSSR **231**, 1335 (1976) [Sov. Phys.—Dokl. **21**, 741 (1976)]; Phys. Status Solidi B **82**, 403 (1977).
[65]T. Damour, in *Proceedings of the First Marcel Grossmann Meeting on General Relativity*, edited by R. Ruffini (North-Holland, Amsterdam, 1977), p. 459.
[66]For $\Omega_{if} < 0$, the lower-branch frequencies are negative, whereas the upper-branch frequencies exceed $E_i/\hbar$. Hence, the anomalous Doppler effect (Ref. 64) cannot occur for frequencies describable by Eq. (39).
[67]A. M. Ozorio de Almeida, Acta Crystallogr. Sect. A **31**, 435 (1975).